FLOOD STUDIES IN TWO CHANNELS WITH A LINK

A Thesis Submitted

in Partial Fulfillment of the Requirements

for the Degree of

Master of Technology

by

KEDAR SHARMA

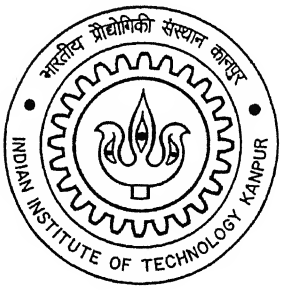

to the

DEPARTMENT OF CIVIL ENGINEERING

INDIAN INSTITUTE OF TECHNOLOGY KANPUR

May, 2005

CERTIFICATE

It is certified that the work contained in the thesis entitled **"Flood Studies in Two Channels with a Link"**, by **Kedar sharma**, has been carried out under my supervision and this work has not been submitted elsewhere for the award of a degree.

(Dr. Rajesh Srivastava)
Associate Professor
Department of Civil Engineering
Indian Institute of Technology Kanpur
Kanpur, India

(Dr. P.K.Mohapatra)
Assistant Professor
Department of Civil Engineering
Indian Institute of Technology Kanpur
Kanpur, India

Dated: May, 2005

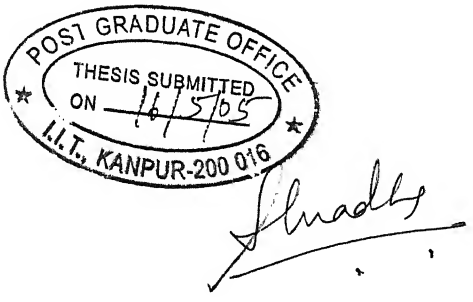

ABSTRACT

Analysis of flood wave propagation is an important engineering practice. In this work, flood wave propagation is studied in two channels with a link. For the purpose, one-dimensional equations for water and sediment flow are considered. A high-order shock-capturing Total Variation Diminishing (TVD) scheme is used for modeling water flow. In addition, the sediment equation is solved by using a different scheme with a semi-coupled approach. This model can simulate either steady or unsteady flows. In case of rigid bed channels, the numerical model is validated against earlier analytical results (Stoker solution) for dam-break flow. However, the present model is validated against experimental results for sediment overloading, in case of mobile channels. The numerical model is applied to two channels with a link to simulate the unsteady flow in both channels. In the absence of experimental data, the results are compared with those obtained from a popular computer package (HEC-RAS). In all the cases, the match between the results is satisfactory and the present model captures the sharp wave front in a better manner. The numerical model is also used to simulate flow distributions in case of flows in rigid bed channels.

ACKNOWLEDGEMENT

I express my deepest gratitude to my thesis supervisor Prof. Pranab Kumar Mohapatra. His wide range experience, enthusiasm, dedication to work and problem solving capacity have enabled me to workout and get through the challenge. I thank him for the exhaustive guidance readily given to me. I am also thankful to my co-supervisor Prof. Rajesh Srivastava.

I wish to express my sincere thanks to my course instructors, Profs. Ashu Jain, Bithin Datta, Bharat Lohani, D. K. Ghosh, and M. S. Kalra for enriching my knowledge in the courses taught by them. I wish to thank some of my seniors Antima, Renu, Anirban Dhar, Sushma, Venu Chandra, Deepesh Singh, Suresh Kartha and Rajmohan Singh for their support.

I wish to thank my entire Hydraulics-group especially Lakshminarayanarao Bachu, Satyendra Pratap Singh, Harikrishna Vennelakanti, Sanjeev K. Jha, Amit K. Diwan, Ch. Sreenivasulu, and Trishikhi, for their help and discussions that I had with them during the M.Tech programme. I also wish to thank my friends Ajay Dashora, Amit Goel, Ravindra Sharma, Sunil Aray, Abhishek Banerjee, Pradyuman K. Shukla, and Shyam Vihari for making my stay at IIT Kanpur enjoyable one. I thank the entire faculty, staff and student community in IIT Kanpur for creating such a nice atmosphere.

I am indebted to my parents, sister and brother-in-law for their blessing and boosting my morale.

I.I.T. Kanpur
May, 2005

(Kedar Sharma)

Dedicated to my grandfather

TABLE OF CONTENTS

Certificate		ii
Abstract		iii
Acknowledgement		iv
Table of contents		vi
List of figures		viii
List of tables		ix
List of symbols		x
CHAPTER I	INTRODUCTION	1
1.1	Review of literature	3
1.1.1	Channel Networks	5
1.1.2	Governing Equations	8
1.1.3	Numerical Methods	9
1.1.4	TVD Scheme	10
1.1.5	ENO Schemes	13
1.1.6	Sediment Modeling	14
CHAPTER II	GOVERNING EQUATIONS	17
2.1	Water flow	17
2.2	Junction flow	20
2.3	Sediment flow	21
CHAPTER III	NUMERICAL SCHEME	23
3.1	Input parameters	26
3.2	Grid parameters	26
3.3	Initial condition	26
3.4	Stability	26
3.5	Unsteady flow calculation	27
3.5.1	Water continuity and water momentum Equation	27

3.5.2	Boundary conditions for Q and A	29
3.5.3	Sediment continuity equation	31
3.5.4	Boundary condition for bed elevation	31
CHAPTER IV	RESULTS AND DISCUSSION	33
4.1	Single channel (rigid bed)	33
4.1.1	Model validation	33
4.1.1.1	Effect of grid size (ΔX)	35
4.1.1.2	Effect of C_n	35
4.1.1.3	Effect of depth ratio	36
4.1.2	Model application	38
4.1.2.1	Steady flow in a single reach channel	38
4.1.2.2	Unsteady flow in a single reach channel	41
4.2	Flow in two channels with link (rigid bed)	44
4.2.1	Model validation	45
4.2.2	Unsteady flow in two channels with link (rigid bed)	47
4.3	Flow in single reach (mobile bed)	52
4.3.1	Model validation	52
CHAPTER V	CONCLUSIONS AND RECOMMENDATIONS FOR FUTURE WORK	55
5.1	Conclusions	55
5.2	Scope for future work	56
Appendix		58
References		60

LIST OF FIGURES

Figure		Page
1.1	Definition sketch: Channel network	6
2.1	Definition sketch: unsteady flow in open channels	19
2.2	Junction conditions	20
3.1	Finite-difference grid	21
3.2	Flow chart for numerical model	25
4.1	Definition sketch: Dam-Break flow	34
4.2	Effect of grid size (C_n= 1.0)	35
4.3	Effect of C_n (Δx = 1m)	36
4.4	Surface profile of DBF due to different depth ratios (Δx = 1m, C_n= 1.0, time=20s)	37
4.5	Results for steady flow in single reach channel	39
4.6	Results for unsteady flow in single reach channel	42
4.7	Definition sketch: two channels with link	45
4.8	Unsteady Flow in Two Channels with Link (Rigid Bed) (Case 1)	48
4.9	Unsteady Flow in Two Channels with Link (Rigid Bed) (Case 2)	50
4.10	Definition sketch: single reach channel (mobile bed)	52
4.11	Effect of sediment overloading	54

LIST OF TABLES

Table		Page
1.1	Example of limiters applicable to solved second- or higher-order numerical schemes for solving conservation laws	11
4.1	Effect of n on flood peak (slope=0.0001)	44
4.2	Effect of bed slope on flood peak (n =0.02)	44
4.3	Summary of results for steady flow in two channels with a link	46
4.4	Effect of link properties on flow in link	47

LIST OF SYMBOLS

A = wetted cross sectional area

B= channel bottom width

C_n=Courant number

c=empirical constant; celerity

d= empirical constant

$e_{1,2}$= eigenvectors

F= flux vector

g= gravitational acceleration

G= source vector

h=flow depth

h_u=upstream water depth in dam

h_d=downstream water depth in dam

i=space node

I_1= hydrostatic pressure force

I_2= pressure force due to width variations

J= Jacobian matrix of flux vector

K= number of divisions

L=left eigen vector matrix, Length of channnel

L_s=splitting operator

m=limiter function

n = Manning's roughness coefficient

n=time node

P = wetted perimeter

p=porosity of bed material

Q = discharge

q_s = total sediment discharge per unit width

R = hydraulic radius; right eigen vector matrix

r=depth ratio

s=sign function

S_0=bed slope

S_f = frictional slope

S_L = side slope (vertical to horizontal)

t = time

U= vector of conservative quantities

u= water velocity

x = horizontal distance along a channel

X=transport parameter

y = water surface elevation

Y=flow parameter

Z = bed elevation

Δt= computational time step

Δx= computational distance step

ε = small positive number

λ=eigen values

CHAPTER I

INTRODUCTION

All human civilizations have been associated with rivers; all major cities in the world are situated on rivers. Therefore, flood studies occupy an important place in engineering application. If the geographical conditions are favorable, then two channels can be linked to transfer the water from one channel to the other. Linking of two channels may help in flood control and in surplus water distribution. In an irrigation system, interlinking of canals is very common.

Many schemes of large scale water transfer projects (interlink proposals) have been planned; some of them are implemented and are standing as a land-mark for the over- all development of the respective regions. In this transfer, water may flow by gravity or by pumping. In Canada, sixteen inter-basin water transfer schemes have been implemented for hydropower development. In USA, the longest and best known schemes implemented so far is California State Water Project, which envisages transfer of water from Sacramento river in North California to southwards through a 715 km long aqueduct with a lift of about 1000 m to meet domestic, industrial and irrigation demands. Similarly, in China, there are schemes existing from ancient times and recently, supplemented by modern construction techniques. China is also planning for transfer of 48 BCM of water from South to North through Grand Canal, close to the Eastern Coast. In India, many interlinking projects were implemented for hydropower and irrigation development. Periyar Project, Parambikulam Aliyar, Kurnool Cudappah Canal, Telugu Ganga Project, Ravi-Beas-Sutlej- Indira Gandhi Nahar Project are some of them. The Sardar Sarovar Project on the river Narmada in Gujarat has successfully linked ten rivers of the state and

has provided a roadmap for the national river-interlinking project. The Narmada Main Canal (NMC), with a capacity to carry 40,000 cusecs of water, has played a major role in channelising the surplus water from the river Narmada to other deficit river basins. A brief note about the interlinking of rivers in India is given in appendix.

If the two channels are linked, the flow is affected in both the channels. The water transferred from one channel may create flood condition in the other. It is also possible that a link makes the water deficiency in the donor channel. After the linking of channels, design of any engineering structure on these two channels is done by taking into account the effect of link on flow. The link also affects the sediment and pollutant transport in the channels.

This problem can be studied by experimental, analytical or numerical modeling (Tannehill et al. 1997). Experimental approach is more realistic than analytical and numerical modeling; however requirement of equipment, scaling problem, measurement difficulties and operating costs are the limitations of experimental modeling. Analytical approach is having the advantages that it has general information in formula form; however; restriction to simple geometry and physics and usually restricted to linear problems are the limitations of analytical approach. The numerical modeling has no restriction to linearity and complicated physics can be treated. Time evolution of flow can be obtained in numerical modeling. Truncation errors, boundary conditions problems and the computer cost are the limitation of numerical modeling. Although, the experimental wok is more realistic, the numerical modeling is used in this study to simulate flow in two channels with link.

In this study, flow in two channels with a link is analyzed for both rigid bed and mobile bed channels. For the purpose, a numerical model is developed to simulate unsteady flow

with shocks. The developed model is then applied to simulate various flood problems: single reach channel (rigid bed), two channels with link (rigid bed), single reach channel (mobile bed) and two channels with link (mobile bed).

1.1 REVIEW OF LITERATURE

Flood routing is described as the procedure whereby the characteristics of a flood wave at one location along a channel are determined from known (or assumed) data at an upstream location (Mahmood and Yevjevich 1975). More generally, routing refers to the mathematical description of water movement (in terms of flow rate or depth), from one location to the other. A flood is most often the result of a volume of runoff entering a channel with in restricted period of time, resulting in a translation wave of long wave length and small amplitude relative to its base length which moves downstream, changing in characteristics as it progresses.

The object of flood flow computation is to determine one or more of the following characteristics of a flood wave:

1. Height –the maximum surface elevation reached; the rate of rise and fall (subsidence) of surface elevation; and the timing involved. Such information is needed in the planning or design of structures across or along streams or rivers.
2. Peak discharge –the maximum volume rate of flow is needed in the design of spillways, bridges, culverts, and channel sections.
3. Total volume of flow –the volume of water involved in a flood is significant in the design and operation of storage facilities for flood control, irrigation, water supply.

4. The area inundated –related to maximum stage, the flood area along any stretch of river is of obvious interest with regard to occupation of flood plains and structure built on them.
5. The timing of flood – question of interest regarding time have to do with the duration of flood conditions and the warning time between the initiation of flood conditions in the channel and the attainment of dangerous or damaging stages at a particular location.

Generally all flood routing techniques require certain data on flow conditions and channel characteristics:

A. Channel characteristics

Topography of reservoir or river and neighboring valley, including contours below normal water level.; Storage volume in a reservoir or stream valley as a function of water surface elevation.; Channel bottom slope, S_o.; Channel cross section at boundaries of the reaches to be used in the model including the flood plain.; Resistance characteristics of the channel in terms of Manning's n, Chezy's C, or conveyance including some evaluation of the variation of resistance with stage.

B. Flow characteristics

Past flow records to establish stage–storage, stage-discharge, and discharge-storage relationship; Measurements or estimates of local overland inflows into the total length of channel, precipitations records, soil moisture indices, runoff characteristics, drainage basic areas, and other hydrologic data involving the rainfall –runoff relationship. Tributary flows may be measured, estimated, or (rarely) determined from a separate routing procedure; Measurements or estimates of the volume inflow to the upper end of

the total channel length as a function of time. Depending upon the technique used, stage verses time data, discharge verses time, or a discharge verses stage curve may be required as a boundary condition or at other location.; Past record of stage-time and/or discharge time data.

1.1.1 Channel Networks

An alignment of channels one the ground is channel network. In open channel flows, there are different types of channel networks as shown in figure 1.1. Choi and Molinas (1993) presented a simulation algorithm for one dimensional unsteady flow routing through channel networks. Khan (1993) presented Muskingum flood routing model for multiple tributaries, in which the Muskingum storage equation was redefined to include the tributary flows as independent inflows to the channel system by increasing the number of x parameters and the routing equation is accordingly modified to contain tributary flows as individual inflows through an increased number of coefficients. Nguyen and Kawano (1995) gave an alternative double-sweeping method applicable to a range of network types. Ji (1998) introduced a different type of discretization scheme for the complete unsteady flow equations and an algorithm to solve these equations for sewer/channel networks with both free surface and surcharged conditions. Ping and Xiaofang (1999) gave a hydraulic flood routing method for multi-Branch Rivers by means of the imaginary channel length using the double-sweeping method. Wu et al. (2004) proposed a one-dimensional model to simulate the nonequilibrium transport of nonuniform total load under unsteady flow conditions in dendritic channel networks with hydraulic structures. The equations of sediment transport, bed changes, and bed-material sorting were solved in a coupling procedure with a direct solution technique, while still the model was decoupled from the flow model. This coupled model for sediment

calculation was more stable and was less likely to produce negative values for bed-material gradation than the traditionally fully decoupled models.

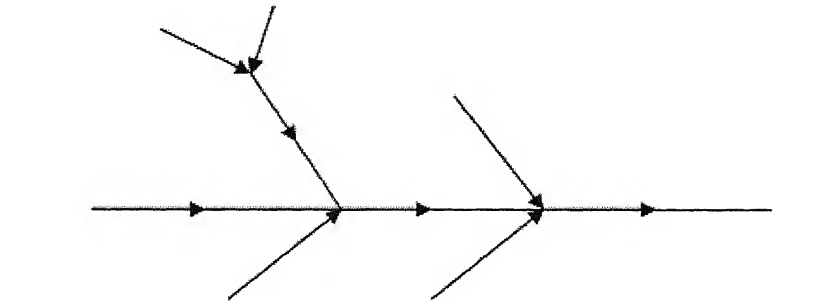

(a)

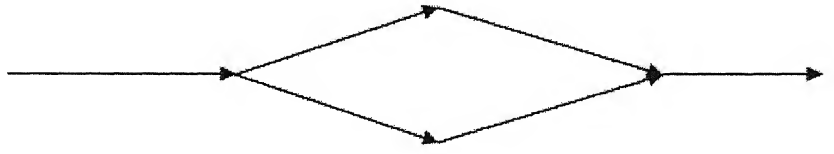

(b)

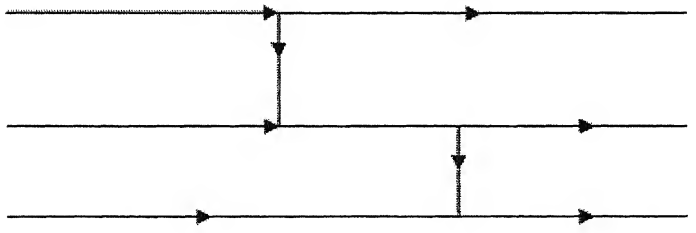

(c)

Figure 1.1: Definition sketch: Channel network

It is seen that most of these schemes are implicit. In an implicit scheme unknown appears in the difference equation in a manner that gives evolution in terms of unknown quantities. It is well known that, although the implicit scheme will yield inherently stable algorithms for the solution of an open-channel network problem, a large number of algebraic equations may have to be solved simultaneously at each time step; as well, a

large number of iterations may be required in order to solve the system at a desired accuracy. Moreover, one still needs to use time steps of the order of the spatial grid size even in an implicit scheme to achieve a uniform accuracy in both space and time discretizations. This is exactly the order of the time step used in an explicit scheme (Aral et al.1998).

To overcome this limitation of implicit schemes, explicit schemes are used in channel networks. In the explicit schemes; only one unknown appears in the difference equation in a manner that permits evolution in terms of known quantities.

Jin and Fread (1997) presented a characteristics-based, upwind, explicit numerical scheme for one-dimensional (1D) unsteady flow modeling of natural rivers and implemented into the U.S. National Weather Service (NWS) FLDWAV model in combination with the original four-point implicit scheme. This explicit scheme was extensively tested and was compared with the implicit scheme. The study showed that the new explicit scheme provided improved versatility and accuracy in some situations, such as particularly large dam-break waves and other unsteady flows with near critical mixed-flow regimes. A technique for implicit-explicit multiple routing to incorporate the advantages of using both the schemes within an application of the FLDWAV model. Aral et al. (1998) presented use of nonoscillatory second order relaxation scheme to simulate the flow in open channel networks. Junction flow conditions in the channel network were solved explicitly using the continuity principle at each junction and the characteristic equations. In that study, flow in two hypothetical channel networks was presented and the model gave satisfactory comparison with widely used Preissmann four-point implicit scheme.

In most of the implicit and explicit schemes, junction conditions are solved by continuity equations and the assumption of equal flow depths at the three or more cross sections of junction. It is shown by Garcia-Navarro (1993) that this is a valid approximation only for few simplified cases. He presented method for surges through an open channel junction and treated the surges through the junction as a hydraulic jump. Assumptions for the method were- the bottom slopes are all zero and the friction is negligible; the channels are of uniform rectangular cross section; only the junction in which two streams combine in a single channel has been considered; the flow is parallel to the channel walls immediately above and below the junction; and the widths of the channels verify: $b_3 = b_1 + b_2$. It may be noted that in the present study, the assumption of equal depths are used.

1.1.2 Governing Equations

To show any physical problem in mathematical form, governing equations are necessary. Different types of governing equations may be used in open channel flows. A three-dimensional fluid flow is represented by the Navier-Stokes equation. Newtonian fluid is the only assumption used in this equation. But the solution of Navier-Stokes equation is not simple: Generally St. Venant equation is used as the governing equation for flow in open channels. Assumptions used in this equation are present in chapter II. Further simplification in momentum term of St. Venant equation results in the kinematic/diffusion equations.

Although, Open channel flows are not always represented by one-dimensional e.g. curved flows, flow at channel expansion, junction flow etc. However, flow is assumed to be one-dimensional in the present study. The sediment transport capacity model consists of the

mass conservation or continuity equations for the water-sediment mixture and bed material (sediment) as well as the momentum conservation equation for the mixture (Cao et al. 2004). By taking the density of water equal to the density of sediment mixture, the continuity and momentum equation for water is not changed as given by St. Venant Equations. Bed elevation change is ignored in the continuity equation for water. Sediment continuity equation is more simplified by eliminating change of rate of sediment density in mixture (Saiedi 1997). For the present study the simplified form of sediment continuity equation (Saiedi 1997) is used.

1.1.3 Numerical Methods

The first attempt to numerically simulate the one-dimensional St. Venant equations for flood routing problems was made by Stoker (1953a) and Isaacson (1954). In 1961, Preissmann provided the famous four-point box scheme. Since than, a variety of numerical techniques have been used to solve flood routing problems. Many of these standard numerical models are discussed or described by Chaudhry (1993). After 1990, a variety of high-order shock-capturing schemes have been used to solve St. Venant equations. Many of these shock capturing models are discussed or described in papers or textbooks (Toro 2001; Zoppou and Roberts 2003). In the present study explicit second order accurate shock capturing TVD scheme in finite-difference approach is used. By changing parameters related to TVD scheme this scheme can be changed to essentially non-oscillatory (ENO) schemes. At the boundaries and junctions the method of characteristic is used.

The functions of continuous argument which describe the state of flow are replaced by functions defined in a finite number of grid points within the considered domain. The

derivatives are then replaced by divided difference. Thus, the differential equations, i.e., the laws describing the evolution of continuum, are replaced by algebraic finite difference relationship. The computational grid is a finite set of points, sharing the same domain in the (x, t) plane.

Most traditional models fail to predict the transcritical flows because of numerical instability. Therefore, High order shock capturing schemes have been extended from the non-linear scalar case to one-dimensional systems, based on the use of Riemann solvers. There is various type of higher-order shock capturing schemes.

1.1.4 TVD Schemes

The concept of TVD scheme was introduced by Harten (1983). The theory which is used to establish a total variation diminishing scheme is based on scalar equations. A measure of the oscillations in a solution is provided by the total variations $TV(U^n) = \sum_{j=-\infty}^{+\infty} | U_j^n - U_{j-1}^n |$ of the grid values U_j at the time level n. Oscillation are avoided if the total variations do not increase with time. A general form of an explicit scheme can be written as

$$U_i^{n+1} = U_i^n - \left(\frac{\Delta t}{\Delta x}\right)\left(\tilde{F}_{i+1/2} - \tilde{F}_{i-1/2}\right) + (\Delta t)\tilde{G}_i^n$$

The numerical flux for the general scheme can be written in the form

$$\tilde{F}_{i\pm1/2} = \frac{1}{2}\left(F_i + F_{i\pm1} + R_{i\pm1/2} D_{i\pm1/2}\right)$$

Where $\boldsymbol{R}_{i\pm1/2}$ is the right-eigenvector matrix corresponding to the approximated Jacobian $\tilde{J}$, and $D_{i\pm1/2}$ is the scheme–dependent vector function. Element of vector $D_{i\pm1/2}$ is

different for different type of scheme (Delis and Skeels 1998). Also the element of vector $D_{i\pm1/2}$ have limiter function applied to the scheme. The purpose of the limiter function is to supply artificial dissipation when there is a discontinuity or a strong gradient, while adding very little or no dissipation in regions of smooth variation. Some of the limiters (Zoppou and Roberts 2003) are given in table 1.1

Table 1.1: Example of limiters applicable to solved second- or higher-order numerical schemes for solving conservation laws

Limiter	$\phi(\beta^+,\beta^-)$
Minmod	$\min\text{mod}(1,\beta^+,\beta^-)=\begin{cases}\min(1,\lvert\beta^+\rvert,\lvert\beta^-\rvert & if\ \beta^+\beta^->0\\ 0 & if\ \beta^+\beta^-\le 0\end{cases}$
Superbee	$\max\left[(0,\min(1,2\beta^-),\min(2,\beta^-)\right]$ $+\max\left[(0,\min(1,2\beta^+),\min(2,\beta^+)\right]-1$
MUSCL	$\max\left\{0,\min\left[2\beta^+,2\beta^-,(\beta^++\beta^-)/2\right]\right\}$
Van Leer	$\frac{\beta^++\lvert\beta^+\rvert}{1+\lvert\beta^+\rvert}+\frac{\beta^-+\lvert\beta^-\rvert}{1+\lvert\beta^-\rvert}-1$
Van Albada	$\frac{\beta^++\lvert\beta^+\rvert^2}{1+\lvert\beta^+\rvert^2}+\frac{\beta^-+\lvert\beta^-\rvert^2}{1+\lvert\beta^-\rvert^2}-1$
Monotonic	$\frac{\beta^++\lvert\beta^+\rvert}{1+\lvert\beta^+\rvert}+\frac{\beta^-+\lvert\beta^-\rvert}{1+\lvert\beta^-\rvert}-2$

Here the $\beta^+=\Delta_{j-1/2}/\Delta_{j+1/2}$, $\beta^-=\Delta_{j+3/2}/\Delta_{j+1/2}$ and $\Delta_{j+1/2}=U_{j+1}-U_j$.

Although application of TVD to nonlinear systems does ensure that the solution will be total variation diminishing, however TVD schemes used to one- dimensional open channel flow equations with source terms, successfully. Garcia-Navarro et al. (1992) used

the TVD-MacCormac scheme for simulating 1-D open channel flow. Delis and Skeels (1998) used the TVD scheme for open channel flows with source terms. The performance of second- and third- order-accurate TVD schemes was investigated for the computation of free surface flows, in predicting dam-break and extreme flow conditions created by the river bed topography. Tseng et al. (2001) presented two high-resolution, shock-capturing schemes for the simulation of 1D, rapidly varied open-channel flows. The scheme presented incorporates the method of characteristics to deal with the unsteady boundary conditions. Also, the Strang-type splitting operator was used to include the effects of bottom slope and friction terms. The results of dynamic flood routing and steady routing was compared to demonstrate the risk of using steady routing for flood mitigation. Burguete and Garcia-Navarro (2001) presented the new technique in which source term was included in the flux limiter functions to get a complete second-order compact scheme. Sanders (2001) presented high-resolution and non-oscillatory solution of the St. Venant equations in non-rectangular and non-prismatic channels. Tseng (2003) presented four different approaches to discretize the source terms for the simulation of one-dimensional open channel flows with rapidly varied bottom topography using TVD-MacCormack-type predictor-corrector scheme. Compared with other high-resolution shock-capturing schemes, MacCormack-type predictor-corrector method is easy to implement and does not presents any additional difficulties in dealing with the source terms. Cao (2004) used TVD scheme for computational dam-break over erodible sediment bed. This paper presented that in early stage of the dam-break, a hydraulic jump is formed around the dam site due to rapid bed erosion, which attenuates progressively as it propagates upstream and eventually disappears. It was also presented that the free surface profiles and hydrographs was greatly modified by bed mobility, which has considerable implications for flood prediction.

1.1.5 ENO Schemes

Shu and Osher (1988) and Nessyahu and Tadmor (1991) proposed the non oscillatory schemes. As presented by Nujic (1995) the simplified version of ENO schemes are presented here. In the ENO scheme the numerical flux is splitted up into two parts

$$F_{j+1/2} = F^{+}_{j+1/2} + F^{-}_{j+1/2}$$

For second-order accuracy numerical fluxes are defined as

$$F^{+}_{j+1/2} = F^{+}_{j} + 0.5\delta F^{+}_{j}$$
$$F^{-}_{j+1/2} = F^{-}_{j+1} - 0.5\delta F^{-}_{j+1}$$

Where

$$F^{+}_{j} = 0.5(F_j + \alpha U_j), F^{-}_{j} = 0.5(F_j - \alpha U_j)$$

Here α represents some positive coefficient, and it is required that

$$\alpha \geq \max_{j} |\lambda_i| \quad \begin{matrix} i = 1,\ldots\ldots,m \\ j = 1,\ldots\ldots,N \end{matrix}$$

m, number of unknowns and N total number of grid points.

The quantities
$$\delta F^{+}_{j} = \min \mathrm{mod}(F^{+}_{j+1} - F^{+}_{j}, F^{+}_{j} - F^{+}_{j-1})$$
$$\delta F^{-}_{j+1} = \min \mathrm{mod}(F^{-}_{j+1} - F^{-}_{j}, F^{-}_{j+2} - F^{-}_{j+1})$$

And each of the fluxes is approximated up to the required order of accuracy.

Tseng (1999) presented the comparison between TVD and ENO schemes. TVD and ENO schemes were shown in a single derivation by using three different parameters. Tseng et al. (2001) presented ENO scheme for the simulation of 1D, rapidly varied open-channel flows. Other high order shock capturing schemes such as upwind schemes (Ying et al. 2004), Relaxation scheme (Jin and Xin 1995 and Aral et al. 1998), flux vector splitting scheme (Jin and Fread 1997), the modified Godunov method (Savic and Holly

1993), the space-time conservation schemes (Chang 1995) and used by Molls and Molls (1998), Lagrangian discrete parcel method (Wang and Shen 1999) and Petrove-Galerking finite elemant scheme (Yang et al. 1993; Khan 2000) were applied to open-channel flows.

Toro (2001) provided an indepth review of TVD schemes and approximate Reimann solvers for the shallow water equations. Zoppou and Roberts (2003) summarized 20 different high resolution shock capturing schemes for dam-break flow and concluded that verity of shock-capturing numerical schemes were efficient, accurate, robust, and suitable for solving the shallow water equations when discontinuities were encountered in the problem. It should be noted that the TVD scheme has second order accuracy, but the characteristic equations which are employed at the boundaries and junctions are only first order. MacCormack heuristically showed that if the order of accuracy of the boundary conditions is an order less than that of interior points, than the overall accuracy of the computed results is not impaired, although other researchers questions the validity of this statement (Fennema and Chaudhry 1986).

1.1.6 Sediment Modeling

In case of water flow in a channel with mobile bed it is require to solve the sediment continuity equation with the water continuity and water momentum conservation equation. There are three different approaches for solving these equations and find the value of flow discharge, area and bed elevation to next time level. In a coupled approach, the physical coupling of water and sediment phases of alluvial flows is recognized and all equations including those related to both water and sediment are solved simultaneously. In the uncoupled approach strong interaction between the bed elevation change and water flow is eliminated. In the uncoupled approach water continuity and water momentum

conservation equation solved simultaneously and the sediment continuity equation is solved separately. If the time step for water flow equation and sediment continuity equation is same in the uncoupled approach, then it is known as semi-coupled model. The main draw back in most uncoupled and semi-coupled models are the assumption of a fixed bed channel when solving flow equations and lack of inclusion of sediment parameters in determining flow resistance.

In many practical cases the use of uncoupled approaches may be justified, mainly because of different time scale in motion of sediment and water, plus the fact that our information on rules of sediment transport and hydraulic resistance in mobile rivers involved empirical relations with various degrees of approximation that largely influence the accuracy of the results from any uncoupled and coupled model. In modeling movable bed channels subjected to peaky floods or strong tidal currents, significant and rapid changes in bed levels, a decoupled model may lead to unacceptable errors in long term prediction of river changes or even to computational difficulties. Saiedi (1994) showed that if the relations used for sediment transport and hydraulic friction in a coupled model are the same as those used in another uncoupled model, the coupled model gives more realistic results. Gill (1983), Nastha et al. (1987), Zhang and Kahawita (1987) and Mohapatra (1991) used decoupled modeling. Mohapatra and Bhallamudi (1994) presented the analytical and numerical model for the analysis of steady-state bed level variation in gradually expanded open channels with movable bed. A second-order accurate, explicit finite-difference scheme (MacCormac scheme) with uncoupled approach had been used by them. Bhallamudi (1991) presented a coupled model for the flow simulation in mobile bed channels. In that study, the MacCormack explicit finite-difference scheme was used which, was second-order accurate, handle shocks and discontinuities in the solution without any special treatment, and allows simultaneous solution of the water and

between results of uncoupled a coupled model. He presented different scheme for discretize the sediment continuity equation and compare with coupled model. Capart and Young (1998) presented the formation of jump by the dam-break wave over a granular bed. In this study a numerical model was present with experimental results and show that shock formation involves a particularly strong coupling between flow free-surface evolution and bed morphodynamics. Cao et al. (2002) presents coupled and decoupled numerical modeling of flow and morphological evolution in alluvial channels. In this study four approaches for water and sediment flow by different simplifications both in water and sediment equations and concluded that it is require fully coupled model is require to simulate extreme flow in channels. Singh et al. (2004) presents a fully coupled one-dimensional alluvial river model for simulation of sharp hydraulic and bed transients in alluvial river. In this study the governing systems of partial differential equations are discretized by making use of generalized Pressmann finite difference scheme. This model is further extended to simulate the process of grain sorting, wash load transport and non-equilibrium sediment transport. Although it is shown that a coupled model is more stable, the semi-coupled approach is used in the present study.

In this chapter, importance of the problem and relevant earlier works are presented. Governing equations are presented in chapter II and their numerical solution is presented in chapter III. Results of the present study are presented in chapter IV. Important conclusions are given in the last chapter. A brief note about interlinking project in India is given in appendix.

CHAPTER II

GOVERNING EQUATIONS

In the present work, flow in two channels with a link is analyzed by using a numerical model. With reference to the present study, governing equations are comprised of continuity and momentum equations for water flow and continuity equation for sediment flow. These equations are described in the following sections.

2.1 WATER FLOW

The fundamental equations of fluid dynamics are based on the following universal laws of conservation: Conservation of mass; Conservation of momentum; and Conservation of energy. However, in this study, only the conservation of mass (continuity equation) and the conservation of momentum laws are used to describe water flow.

For the one-dimensional unsteady gradually varied flow in open channels, continuity and momentum equations (St. Venant 1871; Delis and Skeels 1998; Tseng 1999; Burguete and Garcia–Navarro 2001) are:

Continuity equation;

$$\frac{\partial A}{\partial t}+\frac{\partial Q}{\partial x}=0 \qquad 2.1$$

Momentum equation in longitudinal direction for water

$$\frac{\partial Q}{\partial t}+\frac{\partial(Q^2/A+gI_1)}{\partial x}=gA(-\frac{\partial Z}{\partial x}-S_f)+gI_2 \qquad 2.2$$

In the above equations (2.1 and 2.2), t = time; x = distance along the channel; A = wetted cross-sectional area; Q = volume flow rate; g = gravitational acceleration; Z = bed-

elevation; S_f = friction slope; and I_1 and I_2 represent the hydrostatic pressure force and the pressure force due to width variations, respectively.

The friction slope is calculated using the Manning equation

$$S_f = \frac{n^2 Q^2}{A^2 R^{4/3}} \qquad 2.3$$

In which, n= Manning roughness coefficient and R, hydraulic radius, is the ratio of the cross sectional area, A, and the wetted perimeter, P. The hydraulic radius is equal to the flow depth for wide rectangular channels. Although, n is a complicated function of flow depth, bottom roughness, bed slope, discharge and bed forms, a value independent of these factors are assumed throughout the study.

The hydrostatic pressure force (I_1) is calculated using the following equation

$$I_1 = \int_0^{h(x,t)} (h-\eta) b(x,\eta) d\eta \qquad 2.4$$

and the pressure force due to width variations (I_2) is calculated using

$$I_2 = \int_0^{h(x,t)} (h-\eta) \frac{\partial b(x,\eta)}{\partial x} d\eta \qquad 2.5$$

Where, $b(x, \eta)$ = channel width at depth η; and h = total water depth. For trapezoidal cross sections, I_1 and I_2 are given by

$$I_1 = h^2 (\frac{B}{2} + \frac{hS_L}{3}); \qquad 2.6$$

$$I_2 = h^2 (\frac{1}{2}\frac{dB}{dx} + \frac{h}{3}\frac{dS_L}{dx}) \qquad 2.7$$

Where B = width of channel bottom, and S_L = side slope (vertical : horizontal) of the channel.

Where B = width of channel bottom, and S_L = side slope (vertical : horizontal) of the channel.

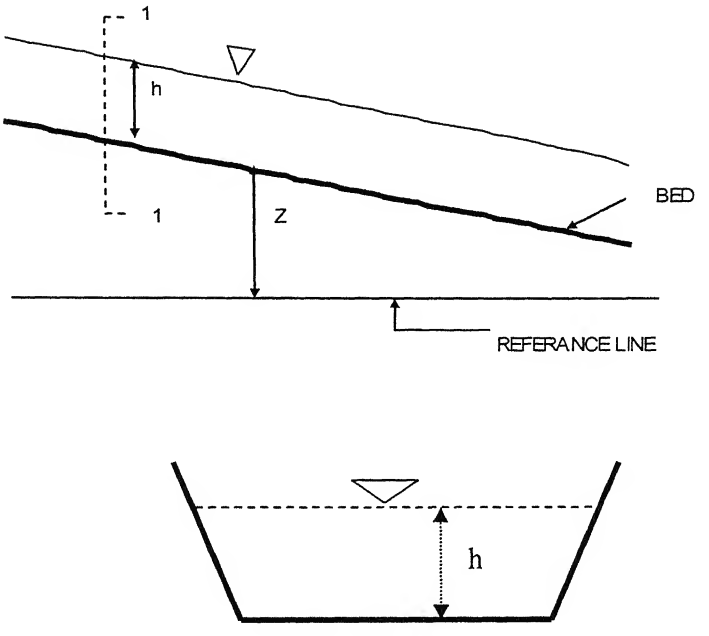

Cross section at 1-1

Figure 2.1: Definition sketch: unsteady flow in open channels

The assumptions used in equations 2.1-2.2 are:

(i) Flow is one-dimensional in all channels. It may be noted that flow at the junction is not one-dimensional due to stream line curvature. However it is assumed to be one-dimensional in this study.

(ii) Slope θ of the channel bottom is small so that $\sin\theta = \tan\theta = \theta$ and $\cos\theta = 1$.

(iii) The pressure distribution at a section is hydrostatic. This is true if the vertical acceleration is small, i.e., if the variation of water surface with alignment is gradual.

(iv) The transient-state friction losses may be computed by using formulas for the steady state friction losses i.e., the roughness coefficient formulas can be used to find the slope of energy line.

(v) The velocity distribution at a channel section is uniform i.e. the velocity is uniform over the cross section and the water level across the cross section is horizontal.

(vi) The channel is straight and prismatic.

Equations 2.1 and 2.2 can be represented in a vector form (Tseng and Chu, 2001) as

$$\frac{\partial U}{\partial t}+\frac{\partial F}{\partial x}=G \qquad 2.8$$

Where, $U=\begin{bmatrix} A \\ Q \end{bmatrix}; F=\begin{bmatrix} Q \\ \frac{Q^2}{A}+gI_1 \end{bmatrix}; G=\begin{bmatrix} 0 \\ gA(S_0-S_f)+gI_2 \end{bmatrix}$

2.2 JUNCTION FLOW

Junctions in a channel network are treated as internal boundary conditions. At the junction, there may be combined or separate flow.

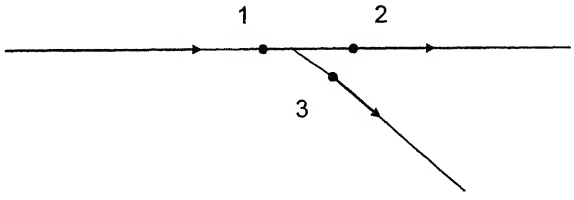

Figure 2.2: Junction conditions

In addition, energy equations between sections 1-2 and 1-3 are also to be satisfied.

$$h_1 + \frac{Q_1^2}{2gA_1^2} + Z_1 = h_2 + \frac{Q_2^2}{2gA_2^2} + Z_2 + h_f \qquad 2.10$$

$$h_1 + \frac{Q_1^2}{2gA_1^2} + Z_1 = h_3 + \frac{Q_3^2}{2gA_3^2} + Z_3 + h_f \qquad 2.11$$

Where h_f is head loss due to friction.

2.3 SEDIMENT FLOW

Like water flow, the sediment continuity and momentum equations are required to represent the sediment flow in channels. Sediment continuity equation can be represented (Saiedi 1997) as:

$$\frac{\partial Z}{\partial t} + \frac{1}{(1-p)}\frac{\partial q_s}{\partial x} = 0 \qquad 2.12$$

Where, q_s = total sediment discharge per unit width, and p = the porosity of bed material.

The sediment flow in a channel is a very complicated phenomenon. The physics of sediment flow is not well understood. Therefore, in place of momentum equation for sediment flow, a simple relationship between the water and sediment discharge is used in addition to the sediment continuity equation (Eq. 2.12), to completely represent the sediment flow. The flow discharge and depth, particle sizes of bed material and bed-forms are the factors on which the sediment discharge depends. Sediment discharge is divided into three parts: bed load, suspended load and wash load. The bed load is the part of sediment discharge which is near the bed and suspended load is the part of sediment discharge in form of suspended material in water. The total load is the summation of the bed load and suspended load. The wash load is generally due to erosion of side walls of channels. The bed load is the major part of the sediment discharge in a channel. Several equations are available for estimating bed load, suspended load, wash load and total load

channels. The bed load is the major part of the sediment discharge in a channel. Several equations are available for estimating bed load, suspended load, wash load and total load in terms of water flow (Graf 1972, Garde and Rangaraju 1985). As suggested by Vanoni (1975) and Jansen et al. (1979) many of these equations can be represented in the following functional form.

$$X = f(Y) \qquad 2.13$$

Where, X is a transport parameter and Y is a flow parameter. The transport parameter depends on the sediment discharge and the grain properties, while the flow parameters depend on the flow properties and the grain size.

For simplicity, the following sediment transport formula is used in this study (Gill 1983, Zhang and Kahawita 1987, Park and Jain 1987, Mohapatra 1991).

$$q_s = c(\frac{Q}{A})^d \qquad 2.14$$

Where, c and d = empirical constants that depend on the sediment properties and the bed forms. This equation is valid only for uniform sediment size. It may be noted that no distinction is made between the bed load and the suspended load and equation 2.14 is assumed to represent the total sediment discharge. The aim of this study is to analyze the flow in two channels with a link. Therefore, the use of a simplified relationship is justified. For real field problems, an appropriate sediment transport equation in place of equation 2.14 should be used.

CHAPTER III

NUMERICAL SCHEME

The continuity and momentum equation for water, and the continuity equation for sediment flow are the governing equations used in this study. The governing equations (2.1 and 2.2) constitute a set of non-linear hyperbolic partial differential equations. In these equations, x and t are the independent parameters; discharge (Q), cross sectional area (A), and bed-elevation (Z) are the dependent parameters. The dependent parameters are known for all x at the initial time level and these are to be calculated for the next time level. Analytical solutions for these equations are available only for idealized cases. Therefore, they are solved numerically. In this study, a finite-difference scheme is used for solve these equations numerically. The functions of continuous argument which describe the state of flow are replaced by functions defined in a finite number of grid points within the considered domain. The derivatives are then replaced by divided difference. Thus, the differential equations, i.e., the laws describing the evolution of continuum, are replaced by algebraic finite difference relationship. The computational grid is a finite set of points, sharing the same domain in the (x, t) plane. A typical computational grid for simple one-dimensional problem is shown in Fig. 3.1. In this study, the governing equations are solved in a semi-coupled approach, i.e. the continuity and momentum equation for water flow are solved simultaneously and discharge and cross-sectional area are used to solve sediment continuity equation.

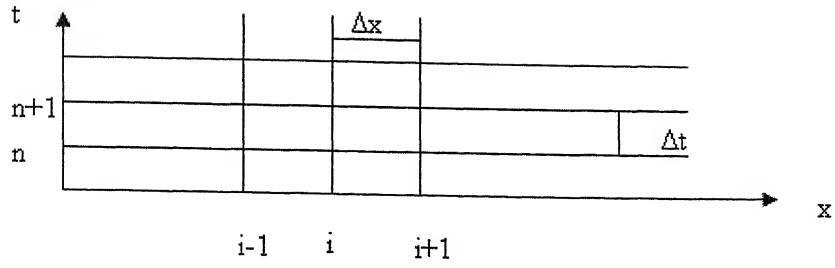

Figure 3.1: Finite-difference grid

In the present study, second order accurate Total Variation Diminishing (TVD) scheme is used to solve the governing equations 2.1 and 2.2. TVD is a high order shock capturing scheme which, numerically captures discontinuities with sharp corners and avoid unrealistic oscillations. For the governing equation 2.8, this algorithm ensures that the total variation does not increase with time, that is:

$$\sum_i |\Delta_{i+1/2} U^{n+1}| \leq \sum_i |\Delta_{i+1/2} U^{n}|$$

Where, $\Delta_{i+1/2}U^n = U^n_{i+1} - U^n_i$. The solution can be second- or third-order accurate in non critical sections, but switches to first order at extreme.

To explain the numerical method, any dependent parameter is expressed as F_i^n, where i and n represent the indices for node number and time level. For example, Q_3^0 is the initial value of discharge at node number 3. As mentioned above, the dependent parameters, at initial time level, are known and it is required to obtain their values at subsequent time levels. The solution strategy is shown in Fig 3.2 and details are provided in the following sections.

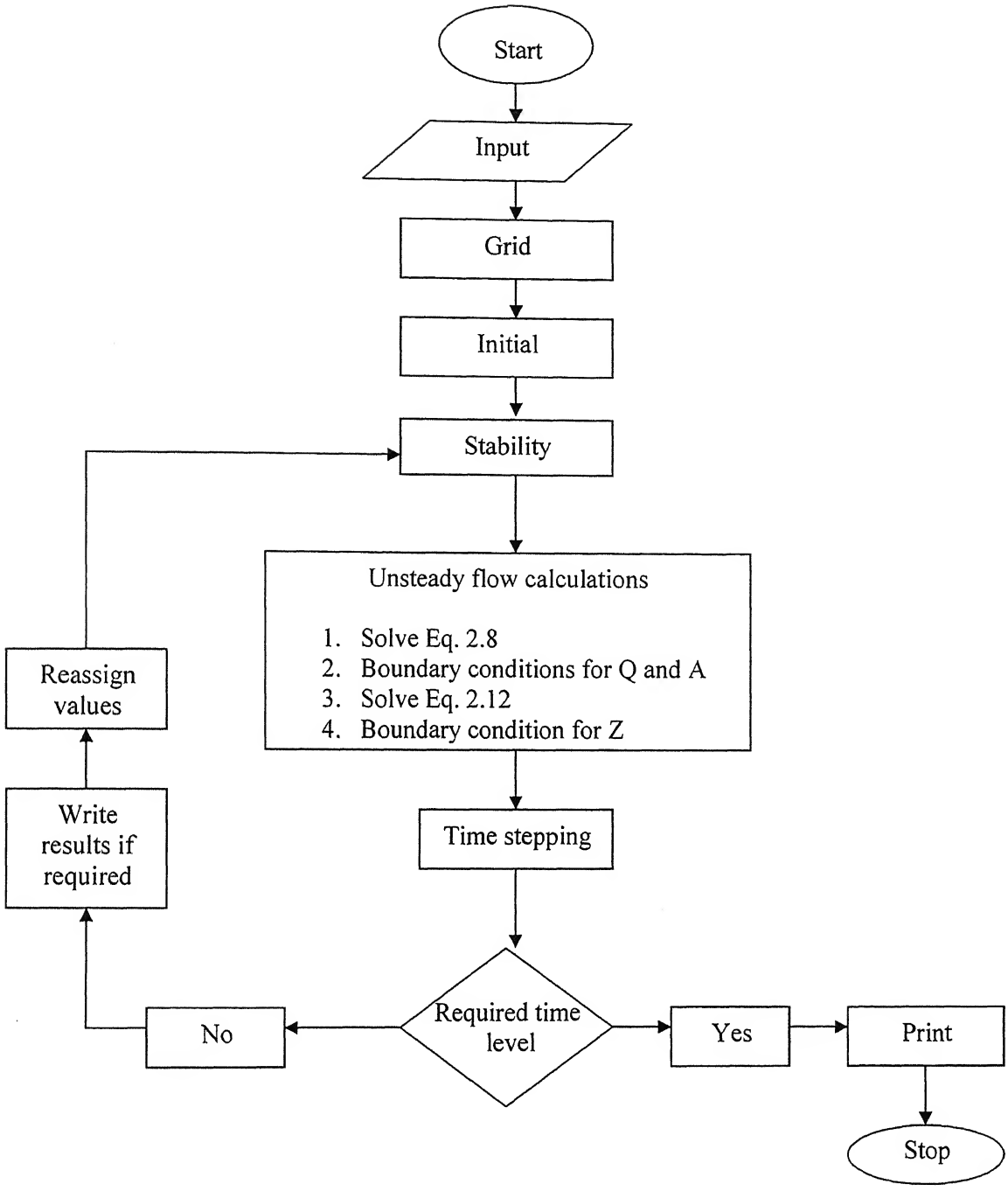

Figure 3.2: Flow chart for numerical model

3.1 INPUT PARAMETERS

The input parameters for the model are cross-sectional geometry, Manning roughness coefficient (n), length of channel L, number of divisions K, acceleration due to gravity (g), porosity of bed material, empirical constants a, c and d (equation 2.14), Courant number (C_n) and time level at which results are required. In addition, the boundary conditions at the inflow and outflow section are given as input.

3.2 GRID PARAMETERS

Δx is given by

$$\Delta x = \frac{L}{K} \qquad 3.1$$

Referring to Fig. 3.1, i_{min}= 1 and i_{max}=K+1.

3.3 INITIAL CONDITION

Initially (t=0) the dependent parameters (Q, A, Z) are either known or are derived from the input parameters.

3.4 STABILITY

For the stability of the present numerical scheme, Courant-Friedrich-Lewy condition is satisfied:

$$\Delta t_i = C_n * \left[\frac{\Delta x}{|\frac{Q_i^n}{A_i^n}| + c_i} \right] \qquad 3.2$$

Where celerity, $c_i = \sqrt{\frac{gA_i}{B_i}}$. Time step, Δt, is chosen as the minimum of all Δt_i.

3.5 UNSTEADY FLOW CALCULATION

3.5.1 Water Continuity and Water Momentum Equation

Total Variation Diminishing (TVD) scheme is used to solve the governing equation 2.8. The homogeneous part of the system is hyperbolic and is responsible for most of the difficulties when it is numerically integrated. The non-linearity of the flux vector $\boldsymbol{F}$ (Eq. 2.8) may lead to spontaneous oscillations, which may have real physical meaning.

For equation 2.8, the flux vector $\boldsymbol{F}$ is related to the flow variables $\boldsymbol{U}$ through the Jacobian $\boldsymbol{J}$ of $\boldsymbol{F}$ with respect to $\boldsymbol{U}$ as

$$\frac{\partial U}{\partial t} + J\frac{\partial U}{\partial x} = 0 \qquad 3.3$$

and

$$J = \frac{\partial F}{\partial U} = \begin{pmatrix} 0 & 1 \\ \frac{gA}{B} - u^2 & 2u \end{pmatrix} \qquad 3.4$$

The hyperbolic nature of the equations ensures that matrix $\boldsymbol{J}$ has a complete set of independent and real eigenvectors, expressed as

$$e^{1,2} = \begin{bmatrix} 1 \\ u \pm c \end{bmatrix} \qquad 3.5$$

In which, velocity $u = \frac{Q}{A}$. The eigen values of $\boldsymbol{J}$ are given by

$$\lambda^{1,2} = u \pm c, \qquad 3.6$$

and correspond to the two characteristic speeds with their signs providing information about the direction of flow. Left and right eigen vectors $\boldsymbol{J}$ is given by $L = \frac{1}{2c}\begin{bmatrix} -\lambda_2 & 1 \\ \lambda_1 & -1 \end{bmatrix}$

and $R = \begin{bmatrix} 1 & 1 \\ \lambda_1 & \lambda_2 \end{bmatrix}$ respectively.

With non-zero source term, Strang-type splitting operator (Strang 1968) is employed to Eq. 2.8 (Seng et al. 2001).

$$U_i^{n+1} = L_s\left(\frac{\Delta t}{2}\right)L(\Delta t)L_s\left(\frac{\Delta t}{2}\right)U_i^n \qquad 3.7$$

Where,

$$L_s(\Delta t)U_i^n = U_i^n + \Delta t G_i^n + \frac{(\Delta t)^2}{2}\left(\frac{\partial G}{\partial U}\right)_i^n (G)_i^n \qquad 3.8$$

and

$$L(\Delta t)U_i^n = U_i^n - \left(\frac{\Delta t}{\Delta x}\right)\left(\tilde{F}_{i+1/2} - \tilde{F}_{i-1/2}\right) \qquad 3.9$$

The numerical flux vector $\tilde{F}_{i\pm1/2}^n$, and the source term averages, $\tilde{G}_i^n$ depends on various schemes. The numerical flux for the general scheme can be written in the form

$$\tilde{F}_{i\pm1/2} = \frac{1}{2}\left(\mathrm{F_i} + F_{i\pm1} + R_{i\pm1/2}D_{i\pm1/2}\right) \qquad 3.10$$

Where $\boldsymbol{R}_{i\pm1/2}$ is the right-eigenvector matrix corresponding to the approximated Jacobian $\tilde{J}$, and $\mathrm{D_{i\pm1/2}}$ is the scheme–dependent vector function.

For TVD2 scheme, the component of $\mathrm{D_{i+1/2}}$ is given as

$$D_{i+1/2}^l = \sigma(\lambda_{i+1/2}^l)\left(e_{i+1}^l + e_i^l\right) - \varphi\left(\lambda_{i+1/2}^l + \gamma_{i+1/2}^l\right)\alpha_{i+1/2}^l, \quad l = 1,2 \qquad 3.11$$

Where,

$$\alpha_{i+1/2} = L_{i+1/2}[\Delta U] \qquad 3.12$$

$$\sigma(z) = \frac{1}{2}\left[\varphi(z) - (\frac{\Delta t}{\Delta x})z^2\right] \qquad 3.13$$

$$e_i^l = m\left[\alpha_{i+1/2}^l, \alpha_{i-1/2}^l\right] \qquad 3.14$$

$$\gamma^{l}_{i+1/2} = \begin{cases} \sigma(\lambda^{l}_{i+1/2})\left(e^{l}_{i+1} - e^{l}_{i}\right)/\alpha^{l}_{i+1/2} & \text{if} \quad \alpha^{l}_{i+1/2} \neq 0 \\ 0 & \text{otherwise} \end{cases} \qquad 3.15$$

The limiter function is given as

$$m(a,b) = \begin{cases} s\min(|a|,|b|) & \text{if sgn a = sgn b = s} \\ 0 & \text{otherwise} \end{cases} \qquad 3.16$$

The entropy correction function is given as

$$\varphi(z) = \begin{cases} |z| & \varepsilon \leq z \\ \left(z^2 + \varepsilon^2\right)/2\varepsilon & \text{if } |z| < \varepsilon \end{cases} \qquad 3.17$$

Here, ε is a small positive number.

3.5.2 Boundary Conditions for Q and A

The model presented in Eq. 3.7 gives the values of Q^{n+1} and A^{n+1} at node 3 to K-1 in a channel. Here, K+1 is the last node of channel reach. For the channel networks, at the junctions Q and A can not be found by TVD scheme; therefore boundary conditions are required.

Open boundaries

The node number 1-2 and K-1 and K are open boundaries for a channel. For node number 1, flow hydrograph or stage hydrograph is the physical boundary condition. For down stream end flow hydrograph, stage hydrograph, normal depth, or rating curve (discharge Vs stage) can be given as physical boundary condition. Other than the physical boundary conditions, characteristic method (Chaudhary 1993, Garcia–Navarro and Saviron 1992, Aral et al. 1998) or some approximation is used to find Q and A at the boundaries (node nos. 1 and K+1).

In method of characteristic (MOC), positive and negative characteristic equations are written as:

$$Q_i^{n+1} = C_p - C_{ai-1} y_i^{n+1} \qquad 3.18$$

and

$$Q_i^{n+1} = C_n + C_{ai+1} y_i^{n+1} \qquad 3.19$$

In which,

$$C_p = Q_{i-1}^n + C_{ai-1} y_{i-1}^n + g(S_o - S_f)_{i-1} \Delta t \qquad 3.20$$

$$C_n = Q_{i+1}^n - C_{ai+1} y_{i+1}^n + g(S_o - S_f)_{i+1} \Delta t \qquad 3.21$$

$$C_{ai} = \left(\frac{g}{c_i^n} \right) A_i^n \qquad 3.22$$

For node numbers 2 and K, two characteristics equations (one positive and one negative) are used to find the values of Q^{n+1} and A^{n+1}. Alternatively, for these nodes condition of node no. 1 and K+1 may be used.

Junction

By referring Fig. 2.2 and applying equation 2.10

$$Q_1^{n+1} = Q_2^{n+1} + Q_3^{n+1} \qquad 3.23$$

Assumption of equal depths at 1, 2 and 3 gives:

$$h_1^{n+1} = h_2^{n+1} = h_3^{n+1} \qquad 3.24$$

Eqs. 3.18 and 3.19 gives

$$Q_1^{n+1} = f(h_1^{n+1}) \qquad 3.25 \text{ (a)}$$

$$Q_2^{n+1} = f(h_2^{n+1}) \qquad 3.25 \text{ (b)}$$

$$Q_3^{n+1} = f(h_3^{n+1}) \qquad 3.25 \text{ (c)}$$

By substituting 3.25 (a), 3.25 (b) and 3.25 (c) in Eq. 3.23 gives a common value h and then by equations 3.25 (a), 3.25 (b) and 3.25 (c) gives three values of Q vales at the junction.

3.5.3 Sediment Continuity Equation

The third dependent variable, Z, is determined at the next time level by solving equation 2.12. As mentioned above, semi-coupled model is used to find the bed level changes, i.e. sediment discharge is found by discharge and depth values and is used to estimate the bed level change in the channel. The following finite difference approximations are used to solve the sediment continuity equation (2.12).

$$\left[\frac{\partial Z}{\partial t}\right]_i = \frac{Z_i^{n+1} - Z_i^n}{\Delta t} \qquad 3.26$$

$$\left[\frac{\partial q_s}{\partial x}\right]_i = \frac{q_{si+1}^{n+1} - q_{si}^{n+1}}{2\Delta x} \qquad 3.27$$

Substitution of equations 3.26 and 3.27 in equation 2.12, gives an explicit equation for Z at the unknown time level,

$$Z_i^{n+1} = Z_i^n - \left(\frac{q_{si+1}^{n+1} - q_{si-1}^{n+1}}{2*(1-p)}\right)\left(\frac{\Delta t}{\Delta x}\right) \qquad 3.28$$

3.5.4 Boundary Condition for Bed Elevation

Equation 3.28 is applicable for points 2 to K. Therefore, Z at node number 1 and K+1 is determined by boundary conditions. In addition for the junctions, it is required to modify the equation. The bed boundary condition is supplied in the form of the known sediment inflow rate as a function of time. In order to express sediment inflow in terms of Z values, the following equation is used (Singh et al. 2004):

$$Z_1^{n+1} = Z_1^n + \left[\frac{(q_{sin}^{n+1} - q_{s1}^{n+1})}{(1-p)}\right]\frac{\Delta t}{\Delta x} \qquad 3.29$$

Where, q_{sin}^{n+1} is the sediment inflow at the unknown time level. Bed level at the downstream end is obtained by extrapolation from the interior points as:

$$Z_{K+1}^{n+1} = 2Z_K^{n+1} - Z_{K-1}^{n+1} \qquad 3.30$$

After determining Q^{n+1}, A^{n+1}, Z^{n+1} for all nodes, time level is increased by Δt. This new time level is compared with the required time level. If the required time level is not reached then reassign the current values of the dependent parameters as the known time level and repeat the earlier steps (Fig. 3.2); else, the computation is stopped depending on the requirement, appropriate printing of the dependent variables is performed.

CHAPTER IV

RESULTS AND DISCUSSION

In the present study, a one-dimensional model using the total variation diminishing scheme (TVD) has been applied to study the flood propagation for two channels with a link. Three different cases, as given below, are studied to meet the objectives

(i) Single channel (rigid bed),

(ii) Two channels with a link (rigid bed),

(iii) Single channel (mobile bed),

Results for these cases are presented below.

4.1 SINGLE CHANNEL (RIGID BED)

Before applying the present model to study flood routing in a single channel, the developed model is validated against the analytical results for dam-break flows (DBF). Because, DBF are with shocks, which provides a check for the shock capturing capabilities of the present methodology (TVD scheme).

4.1.1 Model Validation

The developed mathematical model (as discussed in chapter III) is used to simulate Stoker's solution for dam-break flow (DBF). Stoker (1957) presented analytical results of dam-break flow by using following assumptions: (i) Channel bed is horizontal; (ii) Both reservoir and the channel are infinitely long; (iii) Channel bed and walls are frictionless; (iv) the dam failure is instantaneous; (v) prior to the dam failure, water in both reservoir and the channel is static (Fig. 4.1).

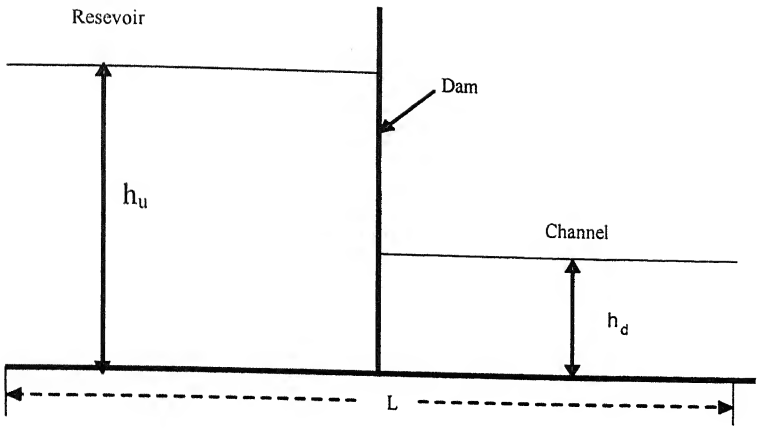

(a) Before the dam-break

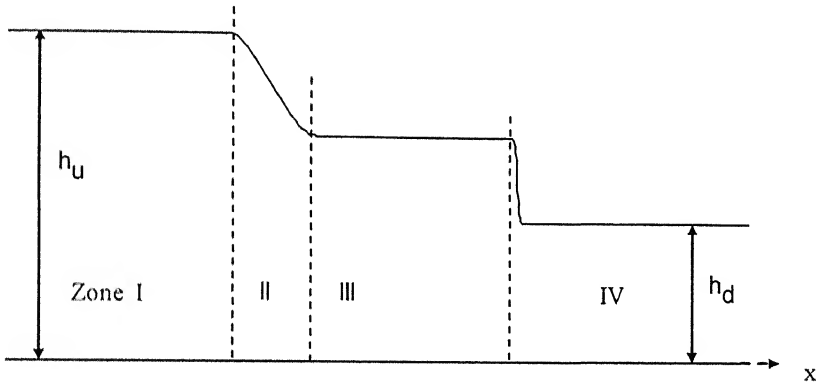

(b) After the dam-break

Figure 4.1: Definition sketch: Dam-Break flow

Different input parameters used for the purpose are: L=1000m; S_0 =0.0; n=0.0; h_u=10.0m; h_d=5.0m and time after dam failure=20s. Numerical parameters such as step size, Δx and Courant number, C_n are varied. It may be noted that these set of input parameters refer to the assumptions used in Stoker's solution. The results indicate four well defined zones in the surface profile after the dam-break. Effects of the various parameters are discussed in the following subsections.

4.1.1.1 Effect of grid size (ΔX)

It is traditional to verify any numerical results for grid independence. The effect of grid size, on the computation of surface profile is presented in Fig. 4.2. Three different values of the step size (Δx=5m, 2m, 1m) is used to find the water surface profile. In this figure, the surface profile is indicated only at the vicinity of the shock.

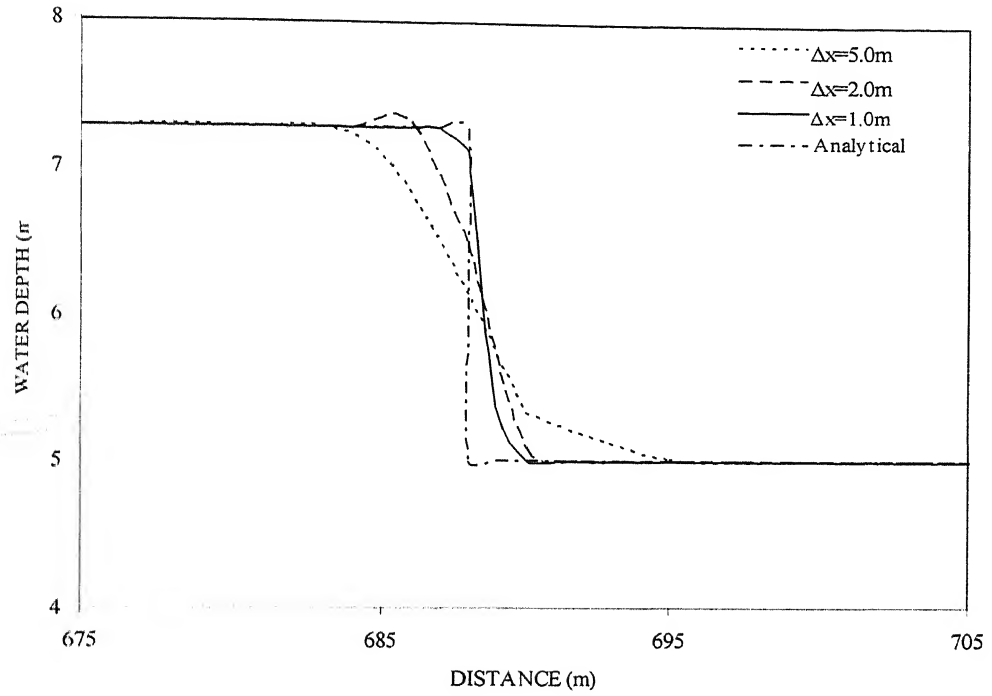

Figure 4.2: Effect of grid size (C_n= 1.0)

As shown in figure 4.2, the best match with the analytical results is predicted by Δx = 1m. Other values of Δx result in smearing of the sharp wave front. Further decrease in grid size does not improve the results significantly.

4.1.1.2 Effect of C_n

Fig 4.3 shows the effect of C_n on the computation of the water surface profile due to DBF.

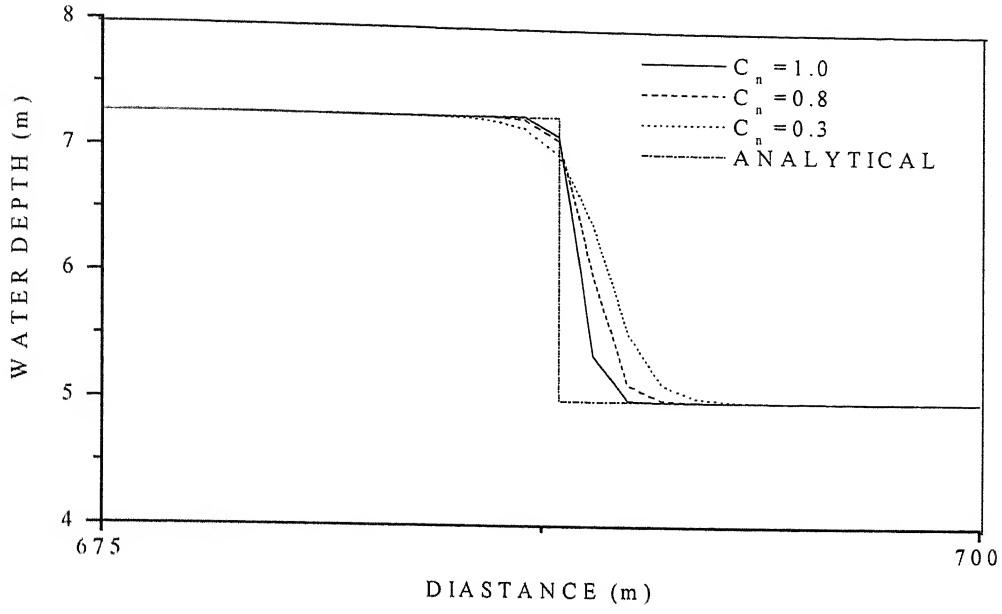

Figure 4.3: Effect of C_n (Δx = 1m)

As shown in Fig. 4.3, a higher value of C_n improves the capturing of the wave front. It may be seen from this figure that even for a value of C_n=1.0 the present model is executable. Therefore, the present model is more efficient compared to other explicit schemes.

4.1.1.3 Effect of depth ratio

Depth ratio, r is defined as the ratio of downstream to upstream depth ($r=h_d/h_u$). In figure 4.4, computed surface profiles by using the present numerical model for three different depth ratios (r=0.5, 0.2 and 0.1) are presented. In all the cases, four zones of Stoker's solution are simulated satisfactorily. As expected the present numerical model captures the sharp wave front very accurately. It is important to note that the present model cannot simulate the DBF for r=0, i.e. a dry bed downstream of dam.

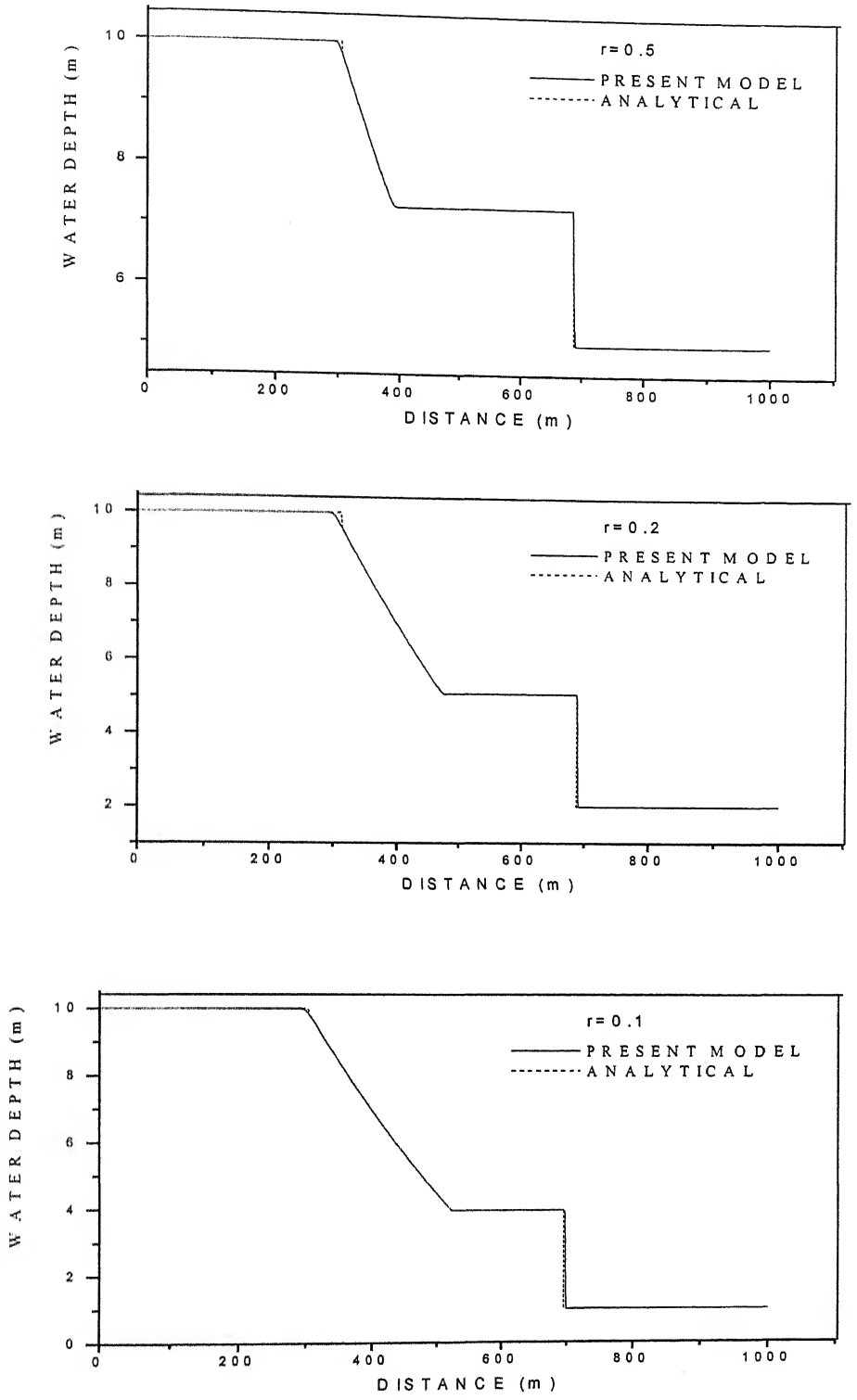

Figure 4.4: Surface profile of DBF due to different depth ratios (Δx = 1m, C_n= 1.0, time=20s)

4.1.2 Model Application

The numerical model presented in the previous chapter and validated in the previous section is used to simulate the flood propagation in a single reach channel. For the single reach channel (rigid bed), results are compared with those obtained from HEC-RAS model (USACE 2005). It may be noted that HEC-RAS is a widely used computer package for flood analysis in open channels.

4.1.2.1 Steady flow in a single reach channel

The present model is used to analyze a steady flow in a single reach channel. The inflow discharge is increased from a constant value of 22.58m^3/s to a higher value of 58.5m^3/s in a very short time period (Fig. 4.5 (a)). The input parameters are L=2000m; B=10m; S_0= 0.0001, C_n=1.0 and Δx=40m. A variable n is estimated by the functional relationship n=0.04-(0.02*x)/2000. The initial discharge and flow depth are taken as 22.58m^3/s and 3.0m, respectively. A normal flow depth is imposed at the down stream boundary. Fig. 4.5 (b), presents the discharge at the out-flow section; Fig. 4.5 (c)-(d) presents variation of the flow depth at inflow and out-flow sections, respectively. In addition, results obtained by using HEC-RAS are also presented in these figures. It may be noted that results are grid independent. As shown in Fig. 4.5, the model obtains a steady state flow condition for discharge 22.58m^3/s and then for 58.5m^3/s. The comparison between present model and HEC-RAS is satisfactory.

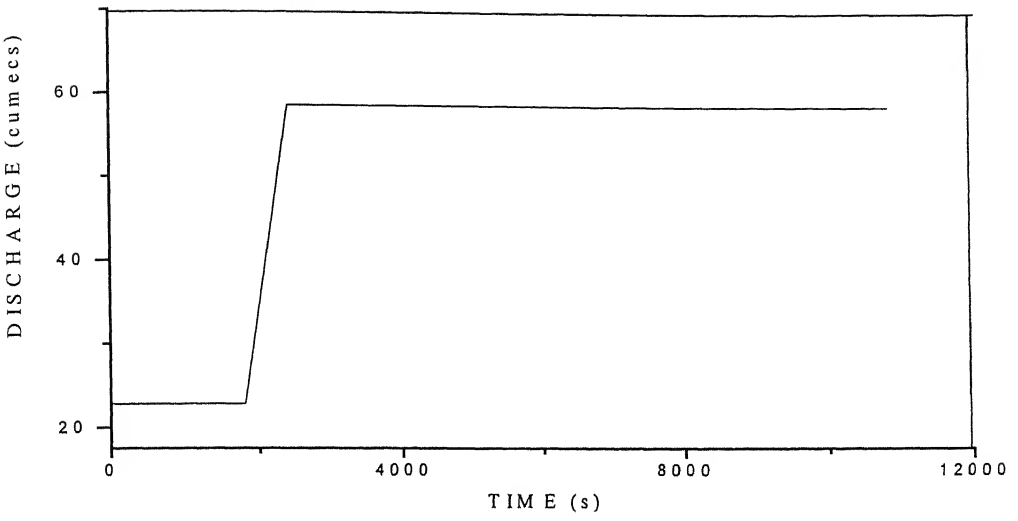

(a) Inflow hydrograph

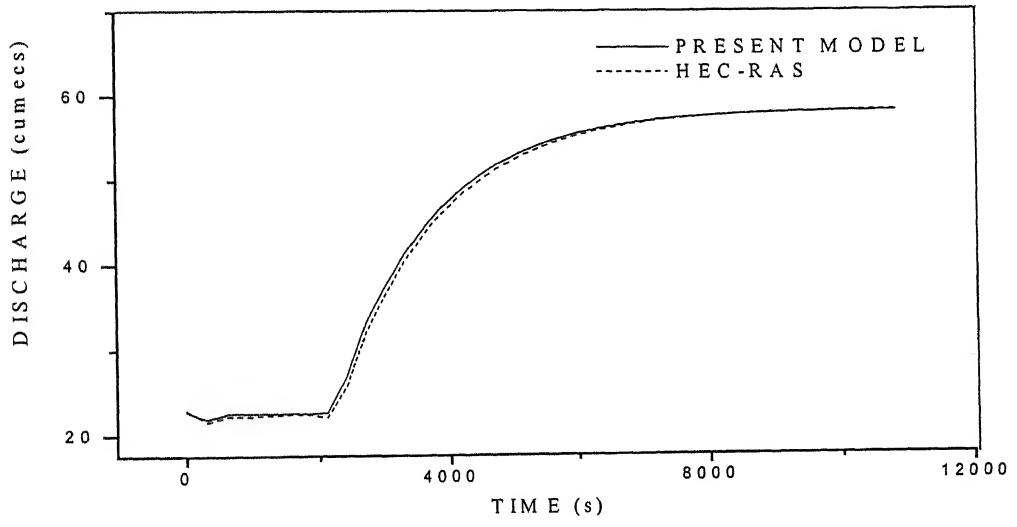

(b) Outflow hydrograph

Figure 4.5: Results for steady flow in single reach

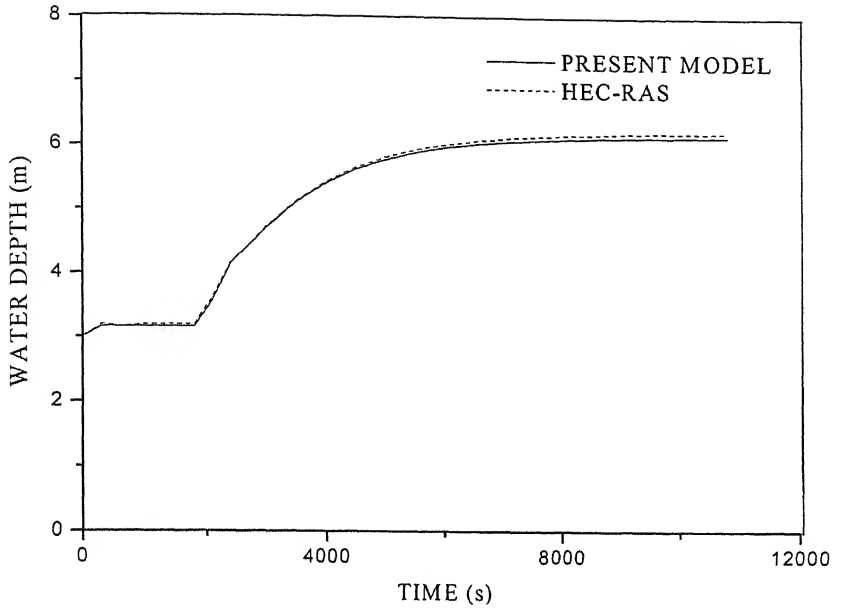

(c) Depth variation at the upstream section

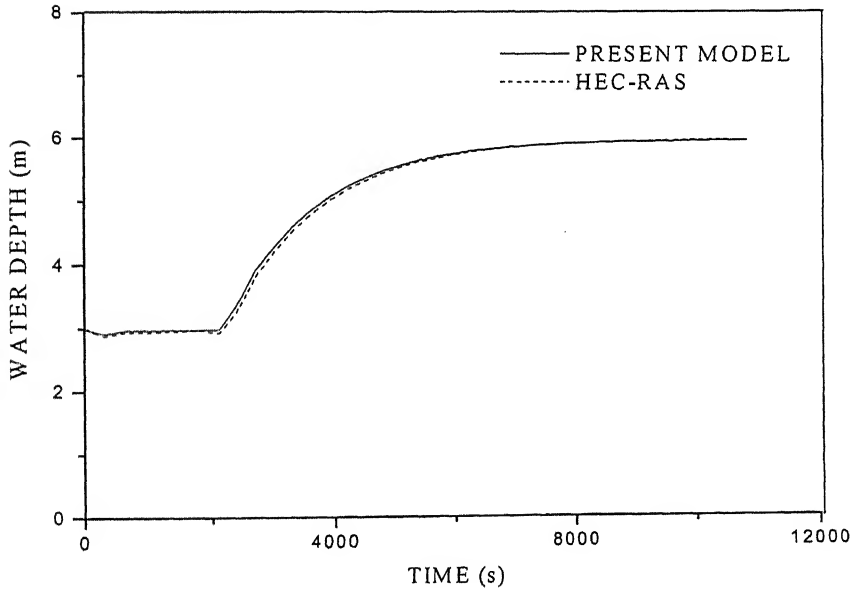

(d) Depth variations at down stream section

Figure 4.5: Results for steady flow in single reach channel (contd.)

4.1.2.2 Unsteady flow in a single reach channel

The present model is used to analyze a flood routing in single reach channel in this subsection. Different input data used are, L=10000m; B=100m; n=0.02; S_0=0.0001. Inflow discharge is $300m^3/s$ up to 3600s, increases to $900m^3/s$ in 3600s and then decreases to initial discharge in 7200s and remain constant (Fig. 4.6 (a)). For simplicity, inflow hydrograph with a triangular shape is used. A normal flow depth is imposed at the down stream boundary. Fig. 4.6 (b) presents depth variation with time at the inflow section (obtained by MOC); Fig. 4.6 (c) presents discharge variation at out-flow section and 4.6 (d) presents depth variation with time at the out-flow section. In addition, results obtained by using HEC-RAS are also presented in these figures. It may be noted that results are grid independent. In Fig. 4.6 (b), there is a difference between depths near the peak value at inflow section. In Fig. 4.6 (c) and (d) there is a fluctuation at the start of rising limb for HEC-RAS model. However, the present model does not have such fluctuation. Probably, it is due to a better shock capturing by the present model. From Fig. 4.6 (a) and Fig. 4.6 (c), there is a decrease in peak discharge from $900m^3/s$ to $625.10m^3/s$ and it is also to be noticed that time to peak at out-flow section is 10807s in comparison of 7200s at inflow section. The overall comparison between the present model and HEC-RAS is satisfactory. Table 4.1 and 4.2 shows the effect of *n* and effect of bed slope on the flood peak and time to peak at the out-flow section. As *n* is increased, peak is reduced and as bed slope is increased the peak is increased.

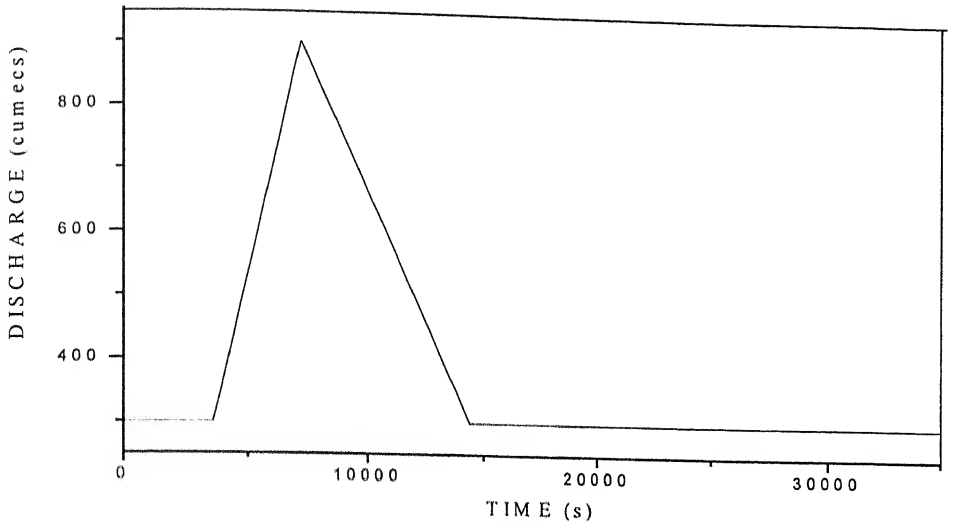

(a) Inflow Hydrograph

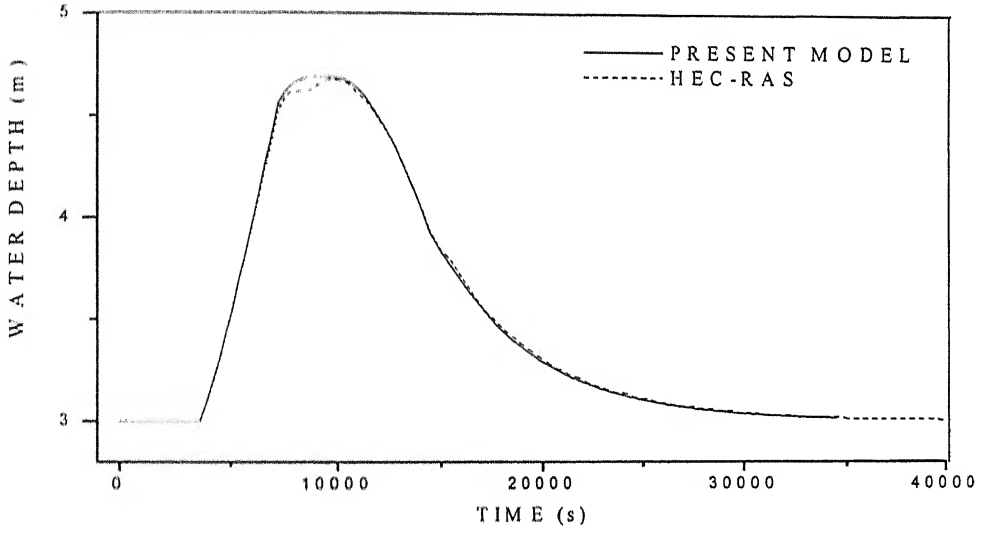

(b) Depths at the inflow section

Figure 4.6: Results for unsteady flow in single reach channel

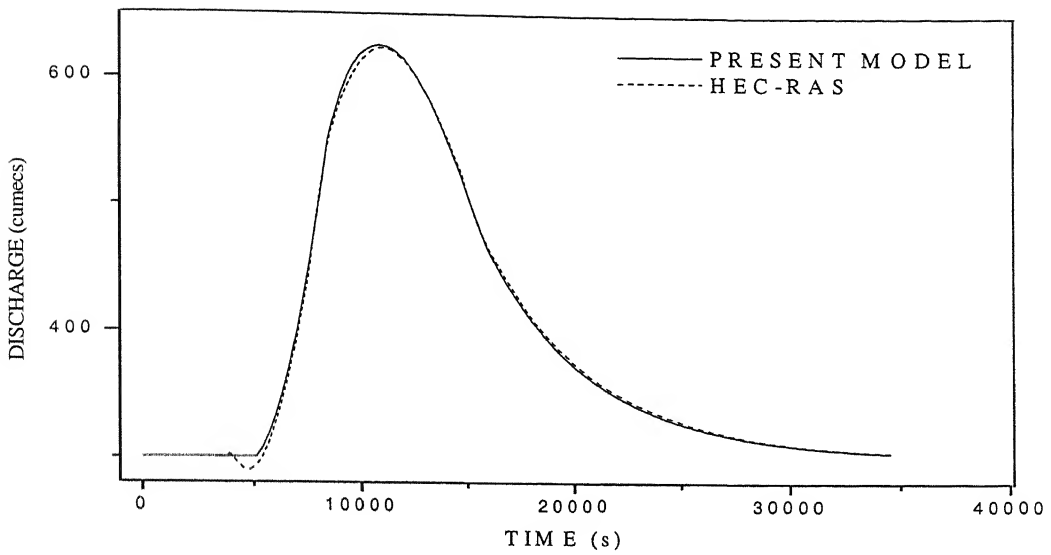

(c) Out-flow Hydrograph

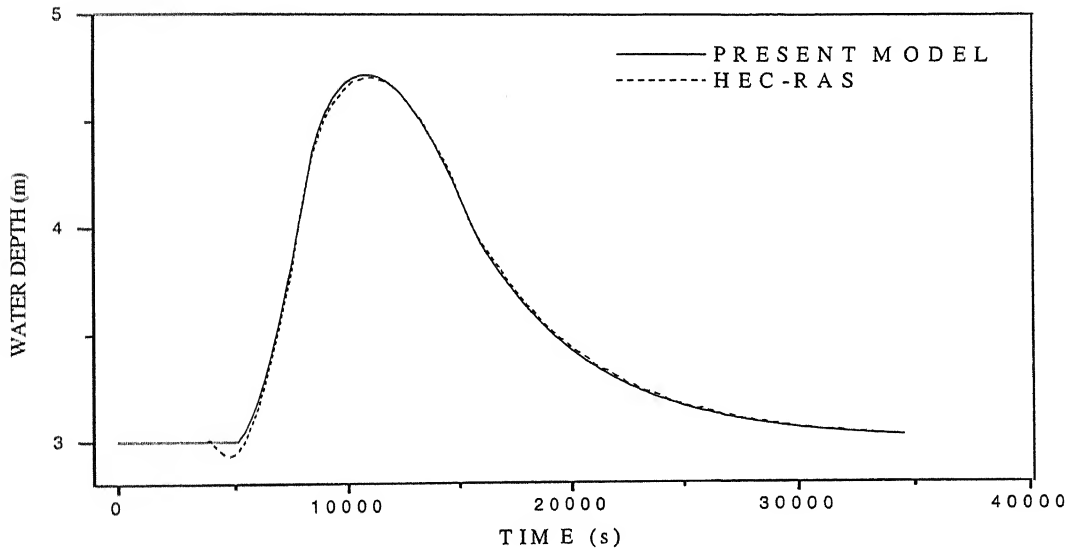

(d) Depth variations at out-flow stream section

Figure 4.6: Results for unsteady flow in single reach (cont.)

Table 4.1 Effect of n on flood peak (slope=0.0001)

Manning's roughness coefficient	Maximum discharge at out-flow section (m^3/s)	Time to peak (s)
0.02	625.1	10807
0.03	580.27	11473
0.04	548.43	11896
0.05	524.73	12219

Table 4.2 Effect of bed slope on flood peak (n =0.02)

Bed slope	Maximum discharge at out-flow section (m^3/s)	Time to peak (s)
0.001	827.95	9332
0.0005	769.94	9874
0.0001	625.1	10807

4.2 FLOW IN TWO CHANNELS WITH LINK (RIGID BED)

Two channels with a link are analyzed in this section (Fig. 4.7). This type of geometry is not common in natural channels. However, it may occur in the following engineering applications as; River networking; Irrigation canal networking; Flow diversion; and Channel splitting.

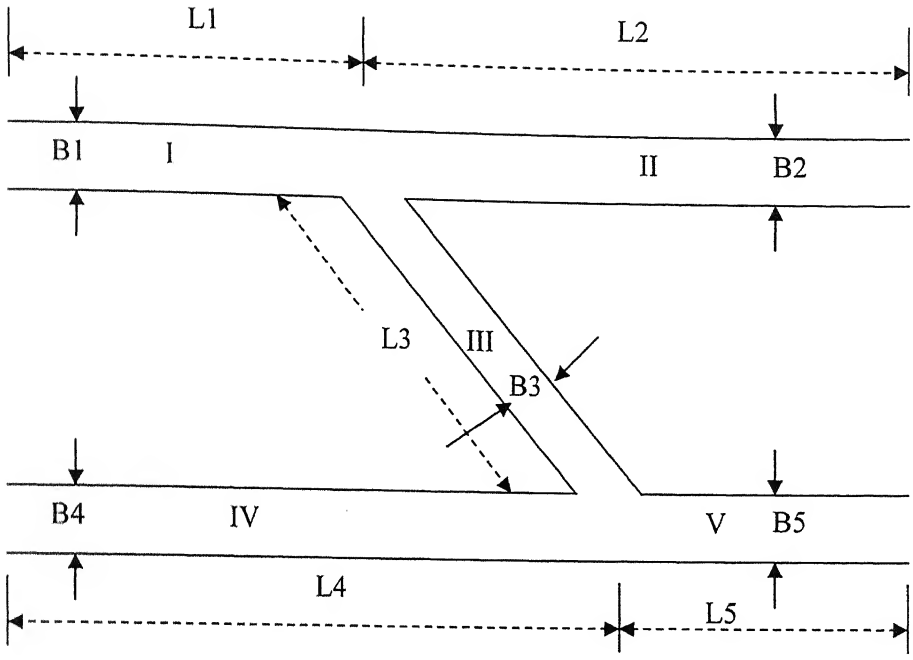

Figure 4.7 Definition sketch: two channels with link

4.2.1 Model Validation

In the absence of any analytical results, the present model is validated against results obtained by using HEC-RAS. Referring to figure 4.7, the input parameters for a hypothetical layout are: L1=L3=L5=4000m; L2=L4=6000m; B1=B2=100m; B3=20m; B4=B5=80m; n1=n2=n3=n4=n5=0.02; $S_01=S_02=0.0005$; $S_04=S_05=0.0005$; Z1=100.0m; Z4=99.0m; Δx=100.0m and C_n=0.8. The constant inflow discharge in channel I and IV is 1000m^3/s and 500m^3/s respectively. The initial depth value used is 3.5m at every location. The results as computed from the present model are presented in table 4.3 in which the nomenclature is used as that discussed in chapter III. In addition, results obtained by using HEC-RAS are also presented in the same table and the comparison is satisfactory.

Table 4.3 Summary of results for steady flow in two channels with a link

Flow parameters in different channels	Present Model	HEC-RAS
$h1_1^n$	3.79 m	3.88 m
$h1_{K+1}^n = h2_1^n = h3_1^n$	3.52 m	3.51 m
$h2_{K+1}^n$	3.56 m	3.51 m
$h4_1^n$	3.76 m	3.71 m
$h4_{K+1}^n = h3_{K+1}^n = h5_1^n$	3.29 m	3.30 m
$h5_{K+1}^n$	4.34 m	4.30 m
$Q3_1^n = Q3_{K+1}^n$	133.08 m^3 /s	134.12 m^3 /s
$Q1_1^n$	1000.00 m^3 /s	1000.00m^3 /s
$Q4_1^n$	500.00 m^3 /s	500.00 m^3 /s
$Q2_{K+1}^n$	866.98 m^3 /s	867.80 m^3 /s
$Q5_{K+1}^n$	633.60 m^3 /s	634.12 m^3 /s

As shown in table 4.3, the flow depths at various points in the channels and link are simulated satisfactorily. A detailed study showing the effects of link parameters on the flow diversion in channel 3 is presented in Table 4.4. Referring to Fig. 4.7 L1=L5=2000m; L2=L4=5000m; B1=B2=100m; B4=B5=60m; n1=n2=0.03; n4=n5=0.02; $S_0$1= $S_0$2=0.0002; $S_0$3=0.0002; $S_0$4= $S_0$5=0.0001; $Q1_1$=1000m^3/s; $Q4_1$=500 m^3/s; Δx=100.0m and C_n=0.8. As shown in table 4.4 the discharge in link is increased with increase length and decrease with increase in *n*.

Table 4.4 Effect of link properties on the flow in link

L3 (m)	W3 (m)	n3	Discharge in link (m^3/s)
1000	20	0.02	81.56
1000	20	0.025	80.31
1000	20	0.03	78.87
1000	20	0.035	77.3
1000	20	0.04	75.62
1500	20	0.03	84.14
2000	20	0.03	88.83
2500	20	0.03	92.88
3000	20	0.03	96.67
4000	20	0.03	102.86
5000	20	0.03	112.36

4.2.2 Unsteady Flow in Two Channels with Link (Rigid Bed)

Eqs. 3.23 and 3.24 are used to solve the flow distribution at a junction. The direction and the quantity of flow in the link are depending on the various channel parameters and flow parameters. In addition, the effect of link on the flood peak depends on the channel parameters and flow parameters. The same geometrical parameters, as in subsection 4.2.1 are used for these cases. Discharge and flow depth at the downstream section are obtained from the characteristic equations and the normal flow condition at this section in both channel II and channel V.

Case 1

For case 1, inflow hydrographs for channel I and IV are given in Fig. 4.8 (a). In fig 4.8 (b), out-flow from channel II is given. In figure 4.8 (c), out-flow from channel V is given. In Fig. 4.8 (b) and 4.8 (c) initial parts show discharge/depth variation due to arbitrary

values. After some time values are set as a steady flow in channels. From Fig. 4.8 (c) it is shown that outflow in channel II reduces for link in comparison to out-flow without link.

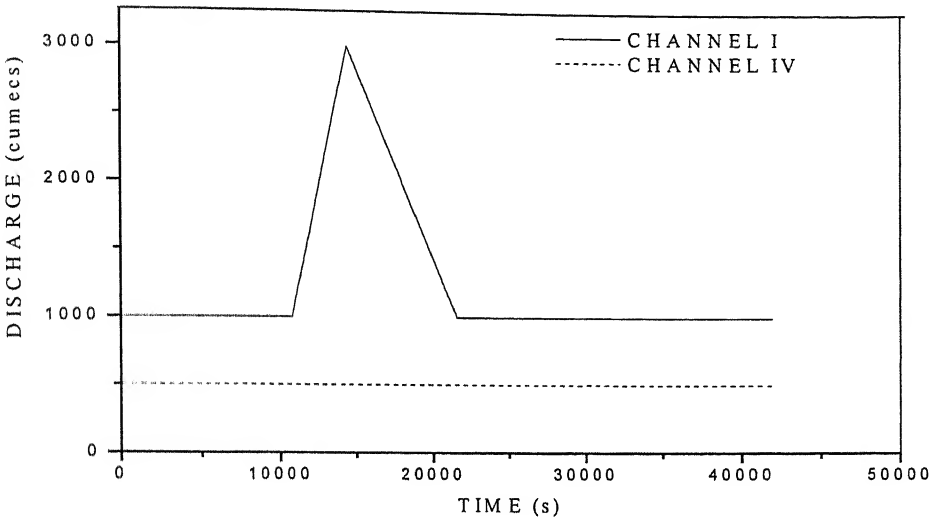

(b) Inflow hydrographs

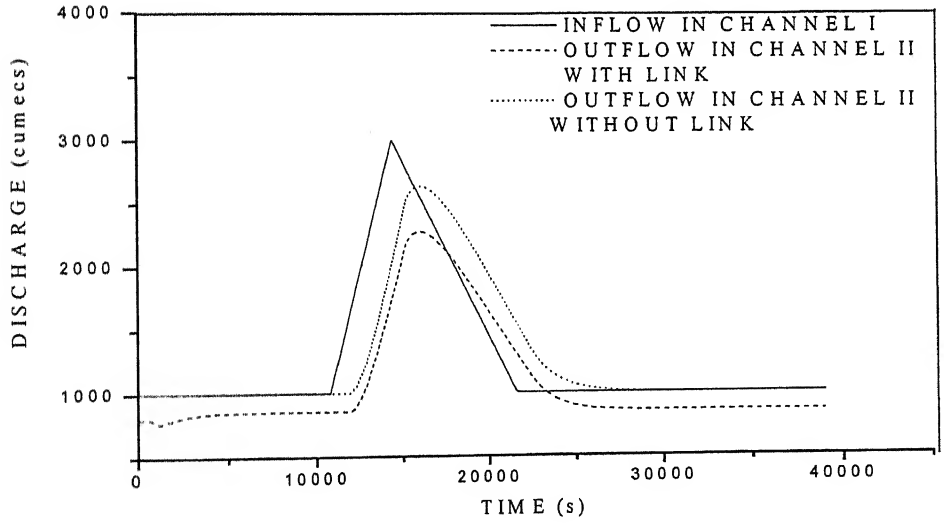

(b) $Q2^{n}_{K+1}$

Figure 4.8: Unsteady flow in 2 channels with a link (rigid bed) (Case 1)

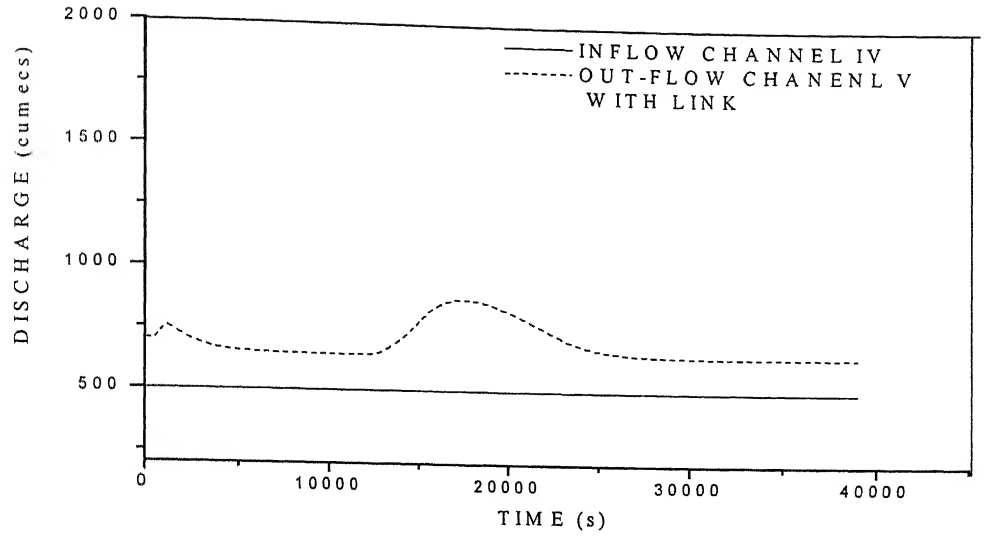

(c) $Q5^{n}_{K+1}$

Figure 4.8: Unsteady flow in 2 channels with a link (rigid bed) (Case1)

(contd.)

Case 2

The inflow hydrographs are shown in Fig. 4.9 (a). Fig. 4.9 (b) and Fig 4.9 (c) shows the outflows in the channel II and V respectively. As shown in Fig. 4.9 (b) outflow discharge for channel II is increased from 855.0m^3/s to 1189.70m^3/s. Fig. 4.9 (c) shows that the peak of outflow in channel V decreased for channels with link. Fig. 4.9 (d) shows the flow in link. In link, flow from channel I to channel V is taken as positive.

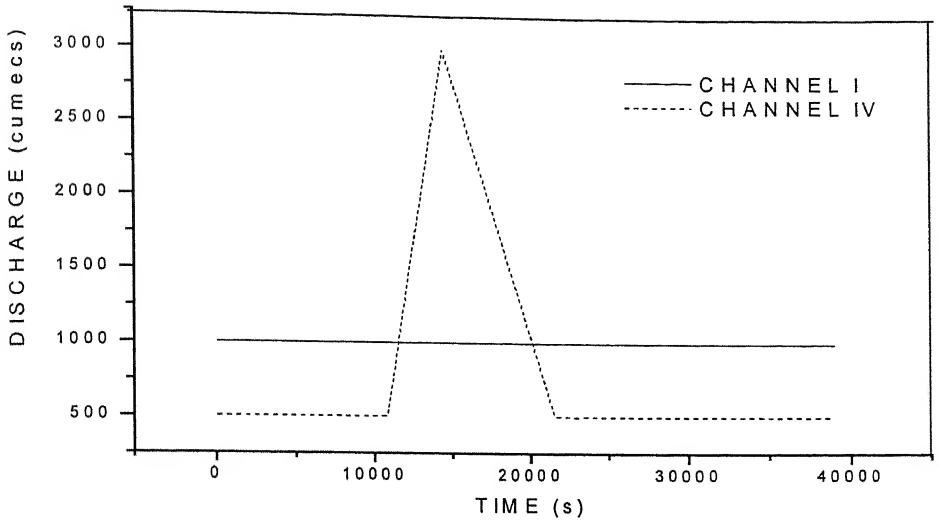

(a) Inflow hydrographs

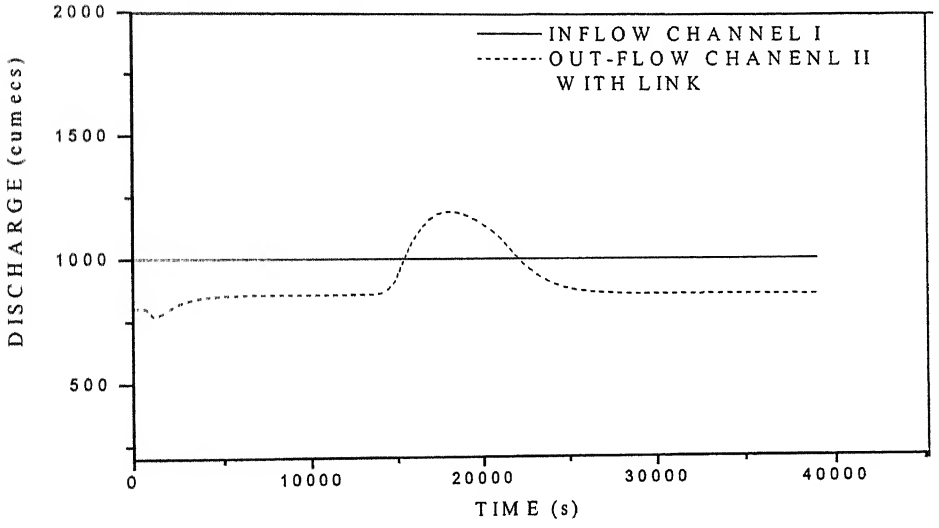

(b) $Q2^{n}_{K+1}$

Figure 4.9: Unsteady Flow in Two Channels with Link (Rigid Bed)

(Case2)

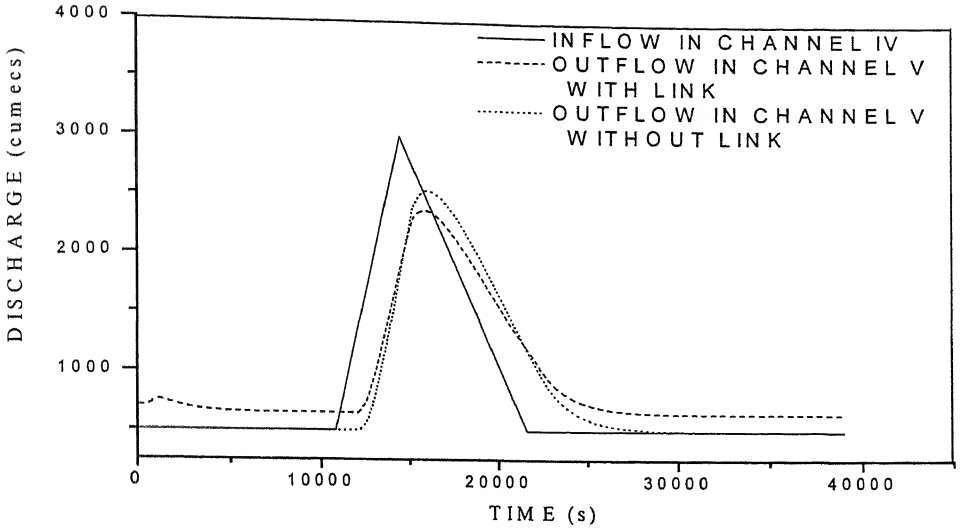

(c) $Q5^{n}_{K+1}$

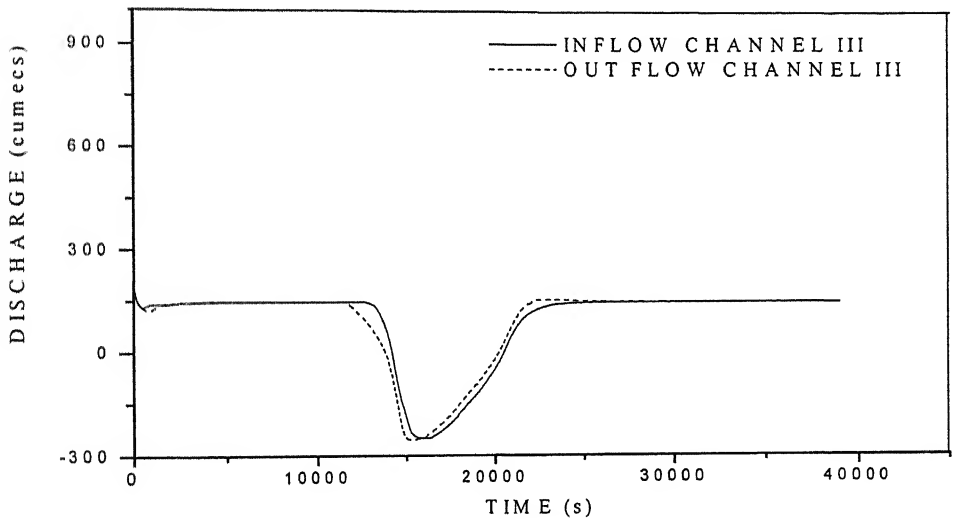

(d) $Q3^{n}_{1} = (\inf low)$ *and* $Q3^{n}_{K+1} = (outflow)$

Figure 4.9: Unsteady Flow in Two Channels with Link (Rigid Bed) (Case 2) (contd.)

4.3 FLOW IN SINGLE REACH (MOBILE BED)

Most of the natural channels are with mobile beds. Many of the man made structures are not properly working or achieving the goal due to lack of information about the sediment transport in channels. Sediment discharge is present due to movable bed; the erosion of side walls or a source of sediment load. As discussed in chapter II, only the bed load is taken in to account in this study. Due to the mobile bed, the flow conditions in channel are changed. As discussed in the previous chapter, the semi-coupled model is used to analyze the flow in a reach with mobile bed. The effect of movable bed on the flow conditions are presented in the following sections.

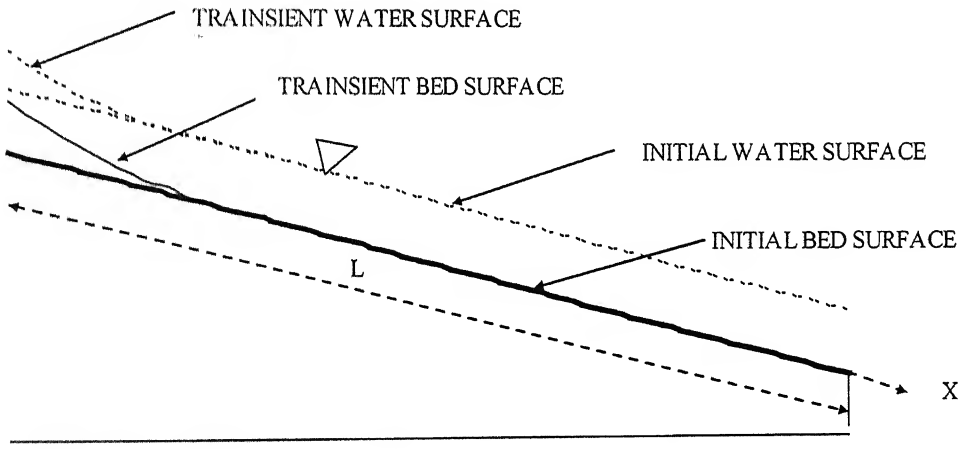

Figure 4.10: Definition sketch: single reach channel (mobile bed)

4.3.1 Model Validation

There is equilibrium for sediment discharge and water flow in a channel. At the inflow section, if sediment inflow is equal to sediment discharge capacity there is no change in bed elevation at inflow section. The sediment over loading is the condition for which the sediment input is more then the sediment discharge capacity (Equation 2. 14). The bed

elevation is changed for the sediment overloading. The performance of the present numerical results for sediment overloading is validated against previous experimental (Soni et al. 1980) and numerical results (Bhallamudi 1991). Referring to the figure 4.10, the input parameters are: L=50m; bed width B=0.2; n=0.02; constant discharge inflow=0.004m^3/s; initial bed slope=0.00356; porosity p=0.4 and initial depth=0.05m. Referring to equation 2.14, empirical constants c = 0.00145 and d=5.0. The grid size, Δx=1.0m and C_n =0.8. These parameters refer to the input values used by Bhallamudi (1991). Bed elevation at the upstream point is estimated by equation 3.27. Discharge and flow depth at the downstream section are obtained from the characteristic equation and the normal flow condition at this section. The bed elevation at the downstream point is determined by extrapolation from the computed values of bed elevation at interior points. Fig 4.11 (a) and 4.11 (b) show the transient bed elevation and water surface, respectively, after 40min of over-loading. It is observed that there is aggradation, up to a distance 15.0m. As shown in figure 4.11 (a) and 4.11 (b) the comparison of bed elevation and water surface is satisfactory. For two channels with a link on mobile bed present model does not give satisfactory results.

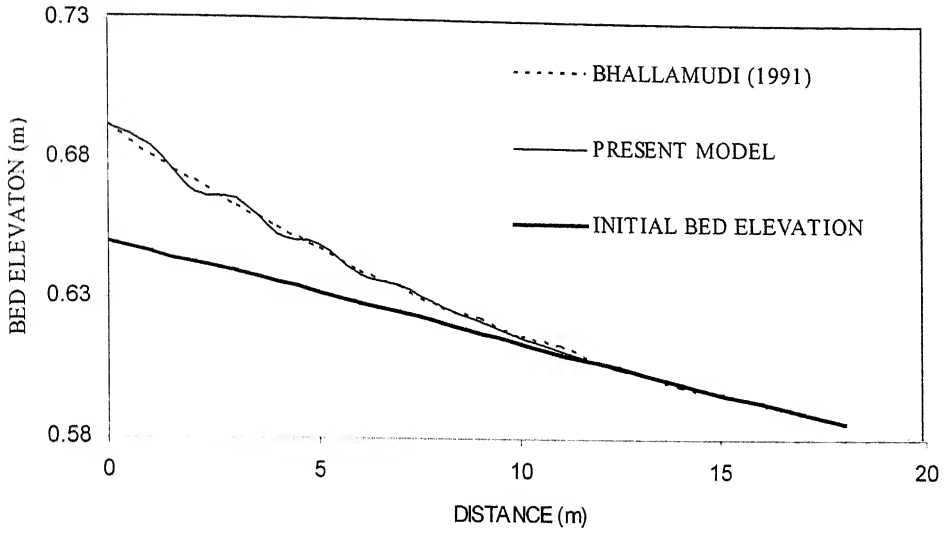

(a) Transient bed profiles at $t = 40$min due to overloading

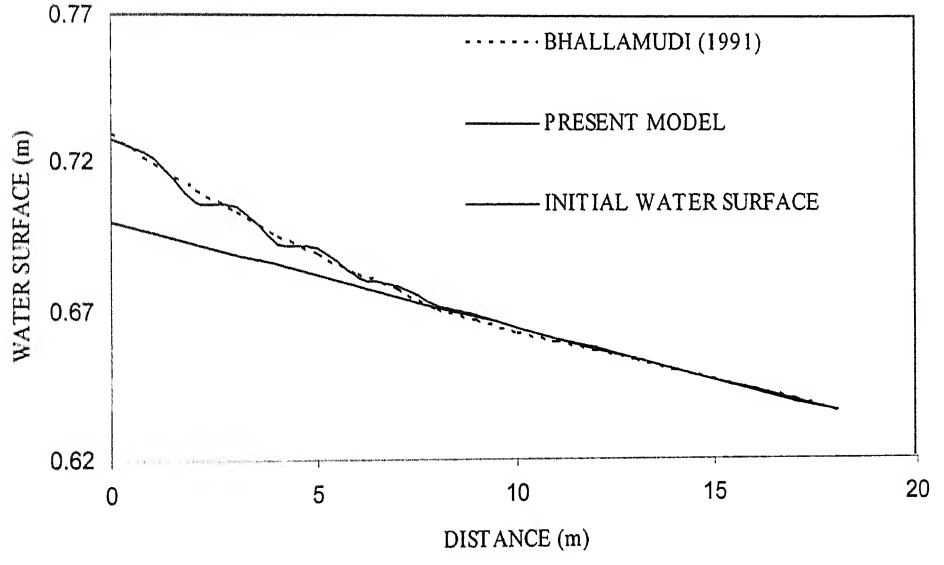

(b) Transient water surface profiles at $t = 40$min due to overloading

Figure 4.11: Effect of sediment overloading

CHAPTER V

CONCLUSIONS AND RECOMMENDATIONS FOR FUTURE WORK

Flood wave propagation in two channels with a link was studied in the present work. A numerical model was developed for the purpose by using the continuity and momentum equations for water flow and continuity equation for sediment flow. The water flow equations were solved numerically by a TVD scheme, where as the sediment flow equation was solved in a semi-coupled manner by a second-order accurate finite-difference scheme. Appropriate boundary conditions for water and sediment flow were imposed at the inflow, outflow and junctions.

Some of the important conclusions of the present study are listed below.

5.1 CONCLUSIONS

The developed numerical model was applied to study the flood wave propagation in

A. Single reach channel with rigid bed;

B. Single reach channel with mobile bed;

C. Two linked channels with rigid bed.

Single reach channel with rigid bed:

1. Strong shocks could be captured by the present model.

2. The maximum discharge at the outflow section decreased with increase in channel bed roughness.

3. The flood wave propagation was faster in case of higher bed slopes.

Single reach channel with mobile bed:

1. Present model could simulate the bed and water surface profile for sediment overloading.
2. Wave like phenomenon was observed for the bed and water surface profiles as compared to earlier experimental and numerical results.
3. This might be due to the semi-coupled approach used in the numerical model.

Two linked channels with a rigid bed:

1. In case of steady flow, flow divisions depended on geometries, flow conditions and bed characteristics of the channels and the link.
2. Assuming the link characteristics as variables, most important parameter influencing the results was length of the link.
3. In case of unsteady flow, maximum outflow in a channel was decreased to 15% when there was no link. However, the outflow was decreased to 30% in the presence of a link.
4. Reverse flow in link could be simulated by the present model.

5.2 SCOPE FOR FUTURE WORK

The present numerical model may be further extended for the followings:

1. In the present study, flow in two linked channels on rigid bed was simulated. This may be extended to two linked channels on mobile bed.
2. Sediment transport equation used in the present model may be replaced by appropriate equation for field conditions.
3. Use of improved surface gradient method for the TVD scheme may be attempted.
4. Coupled modeling for water and sediment flow may be included.

5. Improved junction conditions may be used in the present model.

6. Present model may be modified for application to real life problems.

7. Inverse modeling may be performed for optimal design of the link.

APPENDIX

River interlinking in India

In our country, the rainfall is primarily orographic, associated with tropical depressions originating in the Arabian Sea and the Bay of Bengal. The summer monsoon accounts for more than 85 per cent of the precipitation. The uncertainty of occurrence of rainfall marked by prolonged dry spells and fluctuations in seasonal and annual rainfall is a serious problem for the country. Large parts of Haryana, Maharashtra, Andhra Pradesh, Rajasthan, Gujarat, Madhya Pradesh, Karnataka and Tamil Nadu are not only in deficit in rainfall but also subject to large variations, resulting in frequent droughts and causing immense hardship to the population and enormous loss to the nation. The water availability even for drinking purposes becomes critical, particularly in the summer months as the rivers dry up and the ground water recedes. Regional variations in the rainfall lead to situations when some parts of the country do not have enough water even for raising a single crop. On the other hand excess rainfall occurring in some parts of the country creates havoc due to floods. Irrigation water demand is also increased due to increase in population. It is also require a lot of amount water, which cannot be fulfilled by small-scale irrigation projects. There is a limit to harvest water in small-scale pond, domestic water harvesting unit etc.

One of the most effective ways to increase the irrigation potential for increasing the food grain production, mitigate floods and droughts and reduce regional imbalance in the availability of water is the interlinking of rivers to transfer water from the surplus rivers to deficit areas. If we can build storage reservoirs on rivers and connect them to other parts of the country, regional imbalances could be reduced significantly and lot of benefits by way

of additional irrigation, domestic and industrial water supply, hydropower generation, navigational facilities etc. would accrue. In India 30 links have been identified as technically feasible and economically viable on the basis of pre-feasibility studies. These are: Mahanadi (Manibhadra – Godavari (Dowlaiswaram) link, Godavari (Inchampalli Low Dam) – Krishna link, Godavari (Inchampalli) – Krishna (Nagarjunasagar) link, Godavari (Polavaram) – Krishna (Vijayawada) link, Krishna (Almatti) – Pennar link, Krishna (Srisailam)- Pennar link, Krishna (Nagarjunasagar) – Pennar (Somasila) link, Pennar (Somasila) –Cauvery (Grand Anicut) link, Cauvery (Kattalsi)- Vaigai-Gundar link, Ken-Belwa link, Parbati-Kalisindh-Chambal link, Par-Tapti-Narmada link, Damanganga-Pinjal link, Bedti-Varda link, Netravati-Hemavati link and Pamba-Achankovil-Vaippar link.

Similarly, based on various water balance studies carried out for the Himalayan component, the link proposals identified for preparation of feasibility reports include the Manas-Sankosh-Tista-Ganga link, Kosi-Ghagra link, Ghagra-Yamuna link, Sarda-Yamuna link, Yamuna-Rajasthan link, Rajastan-Sabarmati link, Chunar-Sone Barrage link, Sone Dam – Southern Tributaries of Ganga link, Ganga-Damodar-Subernarekha link, Subernarekha-Mahanadi link, Kosi-Mechi link, Farakka-Sunderbans link, and Jogigopa-Tista-Farakka link.

This national Perspective Plan would give additional benefits of 25 million hectares of irrigation from surface waters, 10 million hectares by increased use of ground water, totaling to 35million hectares which will be over and above the ultimate irrigation potential of 140 million hectares and 34,000 MW of hydro-power apart from the benefits of flood control, mitigation of drought, navigation, domestic and industrial water supply, fisheries, recreational facilities, salinity and pollution control etc

REFERENCES:

1. Aral, M. M., Zhang, Y., and Jin, S. (1998). "Application of relaxation scheme to wave-propagation simulation in open-channel networks." *J. Hydraul. Eng.*, 124(11), 1155-1133.

2. Bhallamudi, S. M. (1991). "Numerical modeling of aggradation and degradation in alluvial channels." *J. Hydraul. Eng.*, 117(2), 1145-1164.

3. Burguete J., and Garcia–Navarro. P. (2001). "Efficient construction of high-resolution TVD conservative schemes for equations with source terms: application to shallow water flows." *Int. J. Numer. Methods Fluids*, 37, 209-248.

4. Cao, Z., Pender, G., Wallis, S., and Carling, P. (2004). "Computational Dam-Break Hydraulics over erodible sediment Bed." *J. Hydraul. Eng.*, 130(7), 689-703.

5. Cao, Z., Day, R., and Egashira, S. (2002). "Coupled and decoupled numerical modeling of flow and morphological evolution in alluvial rivers." *J. Hydraul. Eng.*, 130(7), 689-703.

6. Capart, H., and Young, D. L. (1998). "Formation of a jump by the dam-break wave over a granular bed." *J. Fluid Mech.*, 372, 165–187.

7. Chaudhry, M. H. (1993). *Open-channel flow*. Prentice-Hall, Englewood Cliffs, N.J.

8. Choi, G. W., and Molinas, A. (1993). "Simultaneous solution algorithm for channel network modeling." *Water Resour. Res.*, 29(2), 321–328.

9. Davis, S. F. (1987). "A simplified TVD finite difference scheme via artificial viscosity." *Soc. Indust. Appl. Math. J. Sci. Stat. Comput.*, 8(1), 1-18.

10. Delis, A. I., and Skeels, C. P. (1998). "TVD schemes for open channel flow." *Int. J. Numer. Methods Fluids*, 26, 791–809.

11. Fennema, R. J., and Chaudhry, M. H. (1986). "Explicit numerical schemes for unsteady free-surface flows with shocks." *Water Resour. Res.*, 22(13), 1923–1930.

12. Garcia-Navarro P., Alcrudo F., and Saviron J. M. (1992). "1-D open channel flow simulation using TVD-McCormack scheme." *J. Hydraul. Eng.*, 118(10), 1359–1372.

13. Garcia–Navarro P. (1993). "Surges through an open channel junction." *J. Hydraul. Res.*, 31(1), 79-87.

14. Garde, R. J., and Raju, K.G. R. (1985). *Mechanics of sediment transportation and alluvial stream problems*, 2nd. Ed., Wiley Eastern Ltd., New Dehli, India.

15. Gill, M. A. (1983). "Diffusion Model for Aggrading Channels." *J. Hydraul. Res.*, 21(5), 355-367.

32. Molls, T., and Molls, F. (1998). "Space-time conservation method applied to Saint Venant equations." *J. Hydraul. Eng.*, 124(5), 501–508.

33. Nessyahu, H., and Tadmor, E. (1990). "Non oscillatory central differencing for the hyperbolic conservation laws." *J. Comput. Phys.*, 87, 408-463.

34. Nguyen, Q. K., and Kawano, H. (1995). "Simultaneous solution for flood routing in channel networks." *J. Hydraul. Eng.*, 121(10), 744-750.

35. Nujic, M. (1995). "Efficient implementation of non-oscillatory schemes for the computation of free-surface flows." *J. Hydraul. Res.*, 33(1), 100–111.

36. Park, I., and Jain, S. C. (1986). "River bed profiles with imposed sediment load." *J. Hydraul. Eng.*, 112(4), 267-279.

37. Ping, F., and Xiaofang, R. (1997). "Methods of flood routing for multibranch rivers." *J. Hydraul. Eng.*, 125(3), 271-276.

38. Saiedi, S. (1994). "Numerical and experimental studies of unsteady water and sediment flow in open channels," PhD thesis, School of Civ. Engrg., Univ. of New South Wales, Australia.

39. Saiedi, S. (1997). "Coupled modeling of alluvial flows." *Jour. Hydraul. Eng.*, 123(5), 440-446.

40. Saint Venant, B. (1871). "Théorie de mouvement Non-permanant des eaux avec application aux crues des rivières et à l'introduction des marées dans leur lit." *Acad. Sci.*, Paris, C. R., 73, 148–154, 237–240.

41. Sanders, B. F. (2001). "High-resolution and non-oscillatory solution of the St. Venant equations in non-rectangular and non-prismatic channels." *J. Hydraul. Res.*, 39(3), 321–330.

42. Savic, L. J., and Holly, F. M. (1993). "Dambreak flood waves computed by modified Godunov method." *J. Hydraul. Res.*, 31(2), 187–204.

43. Shu C. W., and Osher S. (1988) "Efficient implementation of essentially Non-oscillatory Shock-capturing Schemes." *J. Comput. Phys.*, 77, 439-471.

44. Singh, A. K., Kothyari, U. C., Rangaraju, K. G. (2004). "Rapidly varying transient flows in alluvial rivers." *J. Hydraul. Res.*, 42(5), 473–486.

45. Soni, J. P., Garde, R. J., and Raju, K.G. R. (1980). "Aggradation in streams due to overloading." *J. Hydraul. Div.*, 106(1), 117-132.

46. Stoker, J. J. (1953). "Numerical solution of flood prediction and river regulation problems." Rep. *II IMM*-200, New York University, New York.

47. Stoker, J. J. (1957). *Water waves, the mathematical theory with applications*, Interscience, London.

48. Strang, G. (1968). "On the construction and comparison of finite difference schemes." *Soc. Indust. Appl. Math. J. Numer. Anal.*, 5(3), 506–517.

49. Tannehill J. C., Anderson D. A., and Pletcher R. H. (1997). *Computational fluid mechanics and heat transfer*, Taylor & Francis, Levittown.

50. Toro, E.F. (2001). *Shock-capturing methods for free-surface shallow flows*, Wiley, New York.

51. Tseng M. H. (1999). "Explicit Finite Volume Non-Oscillatory Scheme for 2D Transient Free-Surface Flows." *Int. J. Numer. Methods Fluids*, 30, 831-843.

52. Tseng, M. H. (2000). "Two-dimensional shallow water flows simulation using TVD-MacCormac scheme." *J. Hydraul. Res.*, 38(2), 123–131.

53. USACE(2005):http://www.hec.usace.army.mil/software/hec-ras/hecrashecras.html

54. Vanoni, V. A. (1975). Sedimentation engineering, *ASCE- Manuals and Reports on Engineering Practice*, no. 54.

55. Wu, W., Vieira, D. A., and Wang, S. Y. (2004). "One-dimensional numerical model for nonuniform sediment transport under unsteady flows in channel networks." *J. Hydraul. Eng.*, 130(9), 914-923.

56. Yang, J. Y., Hsu, C. A., and Chang, S. H. (1993). "Computations of free surface flows. Part 1: One-dimensional dam-break flow." *J. Hydraul. Res.*, 31(1), 19–34.

57. Zhang, H., and Kahawita, R. (1987). "Non-linear Model for Aggradation in Alluvial Channels." *J. Hydraul. Eng.*, 103(3), 913-930.

58. Zhou, J. G., Causon, D. M., Mingham, C. G., and Ingram, D. M. (2001). "The surface gradient method for the treatment of source terms in the shallow-water equations." *J. Comput. Phys.*, 168, 1–25.

59. Zoppou, C., and Roberts, S. (2003). "Explicit schemes for dam-break simulations." *J. Hydraul. Eng.*, 129(1), 11–34.